Report Title: **Enhanced Practical Photosynthetic CO_2 Mitigation**
Type of Report: Final Technical Report

Period Start: 10/02/2001
Period End: 01/02/2006

Principal Authors: Dr. Gregory Kremer, Ohio University
Dr. David J. Bayless, Ohio University
Dr. Morgan Vis, Ohio University
Dr. Michael Prudich, Ohio University
Dr. Keith Cooksey, Montana State University
Dr. Jeff Muhs, Oak Ridge National Laboratories

Date Issued: 01/15/2006
DOE Award No.: DE-FC26-00NT40932

Organizations:

Ohio Coal Research Center
248 Stocker Center
Athens, OH 45701-2979
bayless@ohio.edu
(740) 593 0264 *voice*
(740) 593 0476 *fax*

Department of Microbiology
LW-113B
Montana State University
Bozeman, Montana 59717
umbkc@gemini.oscs.montana.edu

Division of Photonics
Oak Ridge National Laboratory
P.O. Box 2009, MS-8058
Oak Ridge, TN 32831
um4@ornl.gov

Abstract

This final report highlights significant achievements in the Enhanced Practical Photosynthetic CO_2 Mitigation Project during the period from 10/1/2001 through 01/02/2006. As indicated in the list of accomplishments below, our efforts during this project were focused on the selection of candidate organisms and growth surfaces and initiating long-term tests in the bench-scale and pilot-scale bioreactor test systems.

Specific results and accomplishments for the program include:

CRF-2 test system:

- Sampling test results have shown that the initial mass of algae loaded into the Carbon Recycling Facility Version 2 (CRF-2) system can be estimated with about 3% uncertainty using a statistical sampling procedure.
- The pressure shim header pipe insert design was shown to have better flow for harvesting than the drilled-hole design.
- The CRF-2 test system has undergone major improvements to produce the high flow rates needed for harvesting (as determined by previous experiments). The main changes to the system are new stainless steel header/frame units, with increased flow capacity and a modified pipe-end-sealing method to improve flow uniformity, and installation and plumbing for a new high flow harvesting pump. Qualitative system tests showed that the harvesting system performed wonderfully, cleaning the growth surfaces within a matter of seconds.
- Qualitative tests have shown that organisms can be repopulated on a harvested section of a bioreactor screen, demonstrating that continuous bioreactor operation is feasible, with continuous cycles of harvesting and repopulating screens.
- Final preparations are underway for quantitative, long-term tests in the CRF-2 with weekly harvesting.

Pilot-scale test system:

- The construction of the pilot-scale bioreactor was completed, including the solar collector and light distribution system. Over the course of the project, the solar collector used in the light delivery system showed some degradation, but performed well overall.
- Testing confirmed that algae can be grown in a sustainable fashion in the pilot bioreactor, even with intermittent availability of sunlight.
- The pilot-scale tests indicated that algal growth rate followed photon delivery during productivity testing.

Organisms and Growth Surfaces:

- The aeration of growth media with 5% CO_2 in air stimulates cyanobacterial growth 10-20 times over that with air alone. It is possible that the rate of the stimulation of cyanobacterial growth in the CRF will be higher because cyanobacteria will be grown as a biofilm. We plan to increase the concentration to 15% CO_2 in air.
- Tests have shown a doubling time of the cyanobacterial culture of about 7.5 hours with illumination of about 170 μmol m^{-2} sec^{-1}. All lower levels of illumination led to a decrease in the cyanobacterial growth rate.

- Macroscopical and microscopical observations suggest that the culture of this isolate undergoes significant morphological changes after 60-70 hours of incubation in the batch culture mode. First of all, the culture begins to clump. This clumping could lead to the decrease of effective illumination of culture and may reflect a medium alkalinization.
- Organization of our collection of the thermophilic cyanobacteria isolated from Yellowstone National Park has resulted in 13 unialgal cultures of thermophilic cyanobacteria.
- A new species (even probably a new genus) of cyanobacteria, 5.2 s. c. 1, isolated from LaDuke Spring in Great Yellowstone Basin, demonstrates an elevated resistance to some compounds of iron. This might be very important for our project, because plant gases may have elevated amount of iron. Our study of the effect of different concentration of $FeCl_3$ * $6H_2O$ on the growth of the 5.2 s.c.1 isolate showed that iron additions stimulated rather then inhibited the growth of the isolate. Because of this we would recommend this isolate for further experiments.
- The shape of the *Chlorogloeopsis siderophila* cells (cyanobacteria) was found to be affected by environmental pH, which may be useful in culture quality control. Besides, the further investigation of this phenomenon suggested that the rate of cell adhesion to a glass surface decreases upon medium alkalinization. Thus, harvesting effectiveness may be improved by increasing medium pH up to 9 before harvesting of cyanobacteria from a substratum.
- A study of the effects of Omnisil on the growth of 2.1 (III) *Mastigocladus laminosum*, 8.2.1 *Synechococcus* s.c.10, *Chlorogloeopsis* sp. and 3.3.2 *Synechococcus* s.c.1. found that only *Chlorogloeopsis* was able to grow in batch culture in the presence of Omnisil.

Table of Contents

Page

List of Figures

Executive Summary

This final report highlights significant achievements in the Enhanced Practical Photosynthetic CO_2 Mitigation Project during the period from 10/1/2001 through 01/02/2006. As indicated in the list of accomplishments below, our efforts during this project were focused on the selection of candidate organisms and growth surfaces and initiating long-term tests in the bench-scale and pilot-scale bioreactor test systems.

Specific results and accomplishments for the program include:

Test System

- Sampling test results have shown that the initial mass of algae loaded into the Carbon Recycling Facility Version 2 (CRF-2) system can be estimated with about 3% uncertainty using a statistical sampling procedure.
- The pressure shim header pipe insert design was shown to have better flow for harvesting than the drilled-hole design.
- The CRF-2 test system has undergone major improvements to produce the high flow rates needed for harvesting (as determined by previous experiments). The main changes to the system are new stainless steel header/frame units, with increased flow capacity and a modified pipe-end-sealing method to improve flow uniformity, and installation and plumbing for a new high flow harvesting pump. Qualitative system tests showed that the harvesting system performed wonderfully, cleaning the growth surfaces within a matter of seconds.
- Qualitative tests have shown that organisms can be repopulated on a harvested section of a bioreactor screen, demonstrating that continuous bioreactor operation is feasible, with continuous cycles of harvesting and repopulating screens.
- Final preparations are underway for quantitative, long-term tests in the CRF-2 with weekly harvesting.

Pilot-scale Test System

- The construction of the pilot-scale bioreactor was completed, including the solar collector and light distribution system. Over the course of the project, the solar collector used in the light delivery system showed some degradation, but performed well overall.
- Testing confirmed that algae can be grown in a sustainable fashion in the pilot bioreactor, even with intermittent availability of sunlight.
- The pilot-scale tests indicated that algal growth rate followed photon delivery during productivity testing.

Organisms and Growth Surfaces

- The aeration of growth media with 5% CO_2 in air stimulates cyanobacterial growth 10-20 times over that with air alone. It is possible that the rate of the stimulation of cyanobacterial growth in the CRF will be higher because cyanobacteria will be grown as a biofilm. We plan to increase the concentration to 15% CO_2 in air.
- Tests have shown a doubling time of the cyanobacterial culture of about 7.5 hours with illumination of about 170 μmol m^{-2} sec^{-1}. All lower levels of illumination led to a decrease in the cyanobacterial growth rate.
- Macroscopical and microscopical observations suggest that the culture of this isolate undergoes significant morphological changes after 60-70 hours of incubation in the batch culture mode. First of all, the culture begins to clump. This clumping could lead to the decrease of effective illumination of culture and may reflect a medium alkalinization.
- Organization of our collection of the thermophilic cyanobacteria isolated from Yellowstone National Park has resulted in 13 unialgal cultures of thermophilic cyanobacteria.
- A new species (even probably a new genus) of cyanobacteria, 5.2 s. c. 1, isolated from LaDuke Hot Spring in Great Yellowstone Basin, demonstrates an elevated resistance to some compounds of iron. This might be very important for our project, because plant gases may have elevated amounts of iron. Our study of the effect of different concentration of $FeCl_3$ * $6H_2O$ on the growth of the 5.2 s.c.1 isolate showed that iron additions stimulated rather then inhibited the growth of the isolate. Because of this we would recommend this isolate for further experiments.
- The shape of the *Chlorogloeopsis siderophila* cells (cyanobacteria) was found to be affected by environmental pH, which may be useful in culture quality control. Besides, the further investigation of this phenomenon suggested that the rate of cell adhesion to a glass surface decreases upon medium alkalinization. Thus, harvesting effectiveness may be improved by increasing medium pH up to 9 before harvesting cyanobacteria from a substratum.
- A study of the effects of Omnisil on the growth of 2.1 (III) *Mastigocladus laminosum*, 8.2.1 *Synechococcus* s.c.10, *Chlorogloeopsis* sp. and 3.3.2 *Synechococcus* s.c.1. found that only *Chlorogloeopsis* was able to grow in batch culture in the presence of Omnisil.

The result of this project shows that using vertical substrates for growth enhances algal productivity. Further, evidence exists that photosynthetic efficiency is greatly enhanced by photonic distribution. While more testing is needed to optimize the growth of algae in a host flue gas at a specific location (and thus at specific sunlight availability), the results are extremely encouraging that larger-scale applications could be very successful.

It should be noted, however, that one major flaw of this system has been identified. Unless there is a practical use for the resultant biomass, this system is not practical for carbon sequestration. While CO_2 can be removed at a significant level from coal-fired flue gas, the carbon rapidly is re-released as CO_2 as the algal matter decays. Therefore, it is highly suggested that future research focus on the practical conversion of the algal matter to biofuels.

Results and Discussion

Experimental Apparatus

The experimental apparatus used include photosynthetic incubators, bench-scale bioreactors, and a pilot-scale bioreactor that have been previously characterized. Other equipment used includes pipettes, electric balances (mass scales), natural gas burners, $CO/O_2/CO_2$ gas analyzers, and DNA sequencing equipment. Details of the specific applications of the experimental equipment are included in the discussion of the actual data collection and reduction.

Data Collection and Reduction

Task 1.0 Evaluate and rank components and subsystem-level alternative design concepts

Subtask 1.1 Investigate critical properties of alternative photosynthetic agents

1.1.1 Isolation of photosynthetic agents

An analysis of the physico-chemical conditions expected in the Carbon Recycling Facility at Ohio University (CRF) allowed us to envision that the process of photosynthetic mitigation of CO_2 with the help of thermophilic cyanobacteria could proceed at a high temperature (50-60ºC) and at a wide pH range. We began by providing a wide spectrum of photosynthetic agents for examination in the CRF.

1.1.2 Isolation sites

We have carried out sampling in five locations.

1.1.2.1 LaDuke Hot Spring ($44^o05'27"N$; $110^o46'32"W$). This area is shown in Figure 1. The specific properties of this spring are: temperature, 60^oC; pH, 6.85; concentration of iron, 0.4 mg/L, a higher concentration than what is usually found.

Fig. 1. General view of cyanobacterial mat in LaDuke Hot spring. (Pink spots are deposited iron oxide. White rectangles are polymeric traps for cyanobacteria.)

1.1.2.2 Black Sand Pool (44°46'66"; 110°85'18"). This pool, shown in Figure 2, has a very low amount of Ca^{2+} but a high concentration of silica. The temperature was 37-78°C and the pH was 8.8-9.6.

Fig. 2. General view of Black Sand Pool.

1.1.2.3 Angel Terrace in Mammoth Hot Spring area (44°57'59" N; 110°42'37" W). The specific properties of this area, shown in Figure 3, are elevated concentrations of Ca^{2+}, Mg^{2+} and CO_2 in ground water. At the places of sampling the temperature was 40-45°C; pH was 7.5-7.9.

Fig. 3. General view of Angel Terrace slope**.**

1.1.2.4 An unnamed creek in the Rabbit Creek area (44°30'57"N; 110°48'58"W). The specific properties of this area, shown in Figure 4, are: temperature, 51-57ºC; pH, 8.7-8.9. No visible peculiarities of water were observed. However, very obvious cyanobacterial (CB) mats are visible beneath the water surface.

Fig. 4. Unnamed pool in Rabbit Creek area.

1.1.2.5 An unnamed geyser and a fumarole in the West Thumb Geyser Basin. This area is shown in Figure 5. The temperature in the cyanobacterial mat was about 40^{o}C; pH was about 9.8. At the time of sampling the temperature of surrounding water was 75^{o}C; pH was 8.6.

Fig. 5. Unnamed geyser in West Thumb Geyser Basin**.**

The feature in Figure 5 has the shape of small crater with a miniature geyser (or fountain) inside the crater. The height of this geyser is about 30 cm. This crater is surrounded with very strong cyanobacterial mat, which has a rampart shape. The thickness of this rampart reaches up to 25 cm in some places. pH inside the cyanobacterial mat at a depth of about 5 mm was 9.75 – 9.84 despite the fact that the water pH was about 8.4.

1.1.3 Sampling

Sampling was performed in three ways: scraping biomass from a colonized surface, the immersion of some coupons in a water body for *in situ* colonization with cyanobacteria, or the imposition of a coupon on the cyanobacterial mat surface. The surfaces used for *in situ* colonization with cyanobacteria are termed "traps". Several kinds of polymers were used to prepare coupons. They were Scotch Brite™ white and brown felts. Omnisil was used as a substratum for the colonization by cyanobacteria in Angel Terrace, but the geologist of YNP has terminated this experiment. Figures 6 and 7 show a Scotch Brite trap.

Fig. 6. Fresh Scotch Brite trap on the surface of cyanobacterial mat in Black Sand Pool.

Fig. 7. Bottom side of trap after two weeks exposure in Black Sand Pool.

1.1.4 Colonization of traps

All substrata used were firmly colonized by a natural population of cyanobacteria. Figures 8 and 9 illustrate the efficiency of this process on Scotch Brite substratum. The structure of fresh Scotch Brite coupon is shown in Figure 8. Exposure of this coupon in Black Sand Pool leads to a complete colonization of this material (Figure 9). Single fibers of this coupon are no longer visible since all are fully colonized with a cyanobacterial biofilm. Further magnification of this cyanobacterial biofilm suggests that it contains significant diversity.

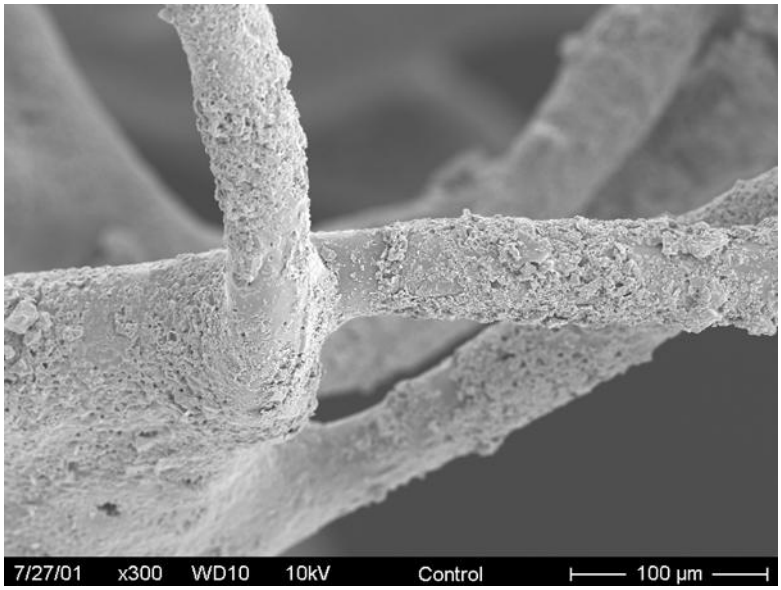

Fig. 8. Single fibers of Scotch Brite under SEM**.**

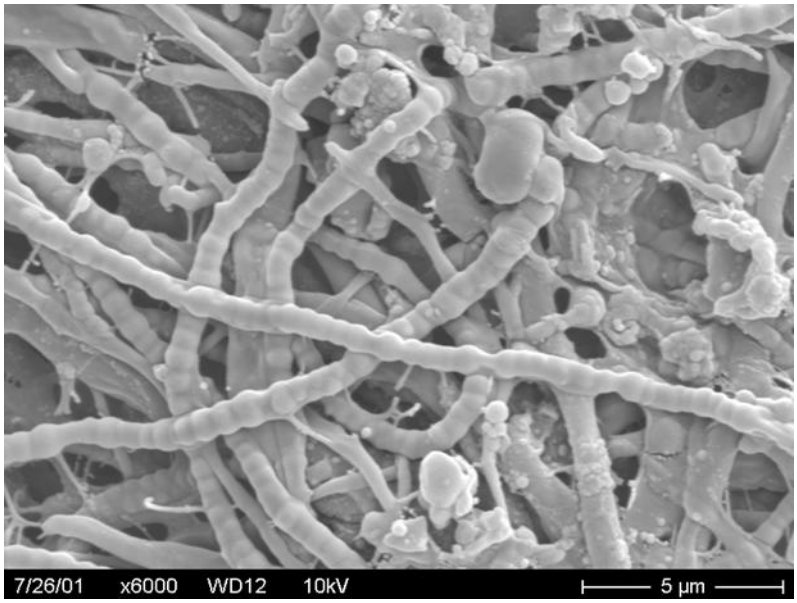

Fig. 9. Natural cyanobacterial biofilm on the surface of Scotch Brite coupon after two weeks exposure in Black Sand Pool**.**

1.1.5 Sample processing

Each sample obtained in the field was divided into three parts. Each sub-sample was immersed into a medium for the cultivation of cyanobacteria. We used three media: BG-11, D and DH. In some cases mixed cultures of cyanobacteria from YNP (i.e. 9.4 Tr4WF) were used.

1.1.6 Isolation of unialgal cultures

Several approaches for the isolation of unialgal cultures have been used. First, we segregated cyanobacterial species using the ability of filamentous CB to move on a semi-solid surface. In particular, isolates s.c.1.2(2), (3), and (6) were obtained by this approach. We also streaked cyanobacterial populations on solidified media. After segregation, single trichomes or unialgal colonies were transferred to small tubes and incubated at 50-55ºC and various light levels. Eventually, these cultures have been adjusted to a volume of about 25-50 mL. Working stock cultures were used at this scale.

1.1.7 Cultivation

Working stock cultures were prepared on scales appropriate for experimentation. However, to study the effect of CO_2 on the growth of thermophilic cyanobacteria, a glass fermenter (bioreactor) was constructed as shown in Figure 10, which maintained a temperature of 55^{o}C.

Fig. 10. General view of glass fermenter**.**

1.1.8 Preservation of photosynthetic agents

Cultures have been preserved according to previously described protocol. Almost all our samples have been frozen in triplicate, at three different concentrations of DMSO: 5%, 10% and 15%. Thus we have accumulated about 500 tubes, which contain about 170 different cyanobacterial samples. These tubes contained general cyanobacterial populations and partially purified and unialgal cultures. As result of this work we have 24 unialgal cultures of thermophilic cyanobacteria. They and their basic properties are listed in Table 1.

Table 1. Details of the current unialgal cultures.

#	Code	Putative name	Place of isolation	Growth Temp.	Shape	Ability to grow in Ca^{2+} medium	Ability to grow with Omnisil
1.	8.2.1 *Phormidium*	*Leptolyngbya*	Angel Terrace	45°C	Filament	+	n.d
2.	8.2.1 "Big trichomes"	*Lyngbya*	Angel Terrace	45°C	Filament	+/-	n.d
3.	8.2.1 *Synechococcus* s.c. (10)	*Synechococcus*	Angel Terrace	55°C	Unicell	-	-
4.	8.1(IV)	*Oscillatoria*	Angel Terrace	45°C	Filament	n.d.	n.d
5.	1.2 s.c. (1)*$	*Chlorogloeopsis*	Rabbit Creek	55°C	Weak filament	+	+
6.	1.2 s.c. (2)*$	*Chlorogloeopsis*	Rabbit Creek	55°C	Weak filament	+	+
7.	1.2 s.c. (3)*$	*Chlorogloeopsis*	Rabbit Creek	55°C	"	n.d	+
8.	1.2 s.c. (6)$	*Chlorogloeopsis*	Rabbit Creek	55°C	"	+	+
9.	1.2 s.c. (8)*$	*Chlorogloeopsis*	Rabbit Creek	55°C	Weak filament	+	+
10.	2.1 *Fischerella*	*Mastigocladus*	Rabbit Creek	55°C	"	n.d.	n.d.
11.	2.1 (III)	*Mastigocladus*	Rabbit Creek	55°C	"	+	-
12.	3.2.2 Low motility fraction *Synechococcus* s.c. (1)	*Synechococcus* sp., C1 type	Rabbit Creek	55°C	Unicell	n.d.	+

13.	3.2.2 Low motility *Syne-chococcus* s.c. (1) + phototax	*Synechococcus* sp., C1 type	Rabbit Creek	55°C	Unicell	n.d.	+
14.	4.1 *Oscillatoria princeps*	*Oscillatoria princeps*	LaDuke (Corwin Spring)	30°C	Filament	n.d.	n.d.
15.	4.1 unicellular	?	LaDuke (Corwin Spring)	30oC	Unicell	n.d.	n.d.
16.	5.2 *Synechocystis*[$]	A representative of new CB genus	LaDuke (Corwin Spring)	55°C	Unicell	n.d.	n.d.
17.	5.2 s.c.1	A representative of new CB genus	LaDuke (Corwin Spring)	55°C	Unicell	n.d.	n.d.
18.	5.2 s.c.2	A representative of new CB genus	LaDuke (Corwin Spring)	55°C	Unicell	n.d.	n.d.
19.	5.2 s.c.3	A representative of new CB genus	LaDuke (Corwin Spring)	55°C	Unicell	n.d.	n.d.
20.	5.2 s.c.4	A representative of new CB genus	LaDuke (Corwin Spring)	55°C	Unicell	n.d.	n.d.
21.	5.2 s.c.5	A representative of new CB genus	LaDuke (Corwin Spring)	55°C	Unicell	n.d.	n.d.
22.	8.2 BF	n.d.	Angel Terrace	45ºC	?	+	n.d.
23.	8.2.1 Tr. Cord 5 months s.c. 10 *Synechococcus*	*Synechococcus* sp. C9 type					
24.	4.1 D unicell	n.d.	LaDuke	45ºC	Unicell	n.d.	n.d.
25.	3.2.2 low motility s.c.1 positive	*Synechococcus* sp.,C1 type	Rabbit Creek Area	55°C	Unicell	n.d.	+

n.d. : Not determined

* sent to Ohio University

[$] Isolate from wall mat. It means that this organism can grow in an atmosphere of hot steam. "Weak filament" means that this organism is a chain former.

1.1.9 Growth

1.1.9.1 Growth characteristic of different isolates. The first attempted saturation of BG-11 medium with 5% CO_2 produced a measurable decrease in cyanobacterial growth, when compared with atmospheric levels of CO_2. Saturation with CO_2 led to acidification of the growth medium. BG-11 medium with the addition of 5 mM $NaHCO_3$ was then used as a buffer, where $NaHCO_3/CO_2$ allowed the pH of the medium to remain at about pH 8. In later experiments, 0 mM N-(2-hydroxyethyl) piperazine-N`-(2-ethanesulphonic acid (HEPES) buffer was used. This approach maintained pH at the desired level for several months.

The growth properties of different CB isolates from YNP are shown in Figure 11. In first series of experiments, the rate of growth of six isolates (in 50mL BG-11 medium supplemented with 5% of $NaHCO_3$ and aerated with 5% of CO_2) was determined. The rate of gas flow was 6-8 mL/min. The level of illumination was about 75 $\mu Em^{-2} sec^{-1}$. Note that it was not possible to measure the irradiance inside the bioreactors so the incident irradiance is quoted. Growth is reported in arbitrary fluorescence units derived from a methanol extract of the cells. The doubling time for this group of isolates varied between 8 and 19 hours.

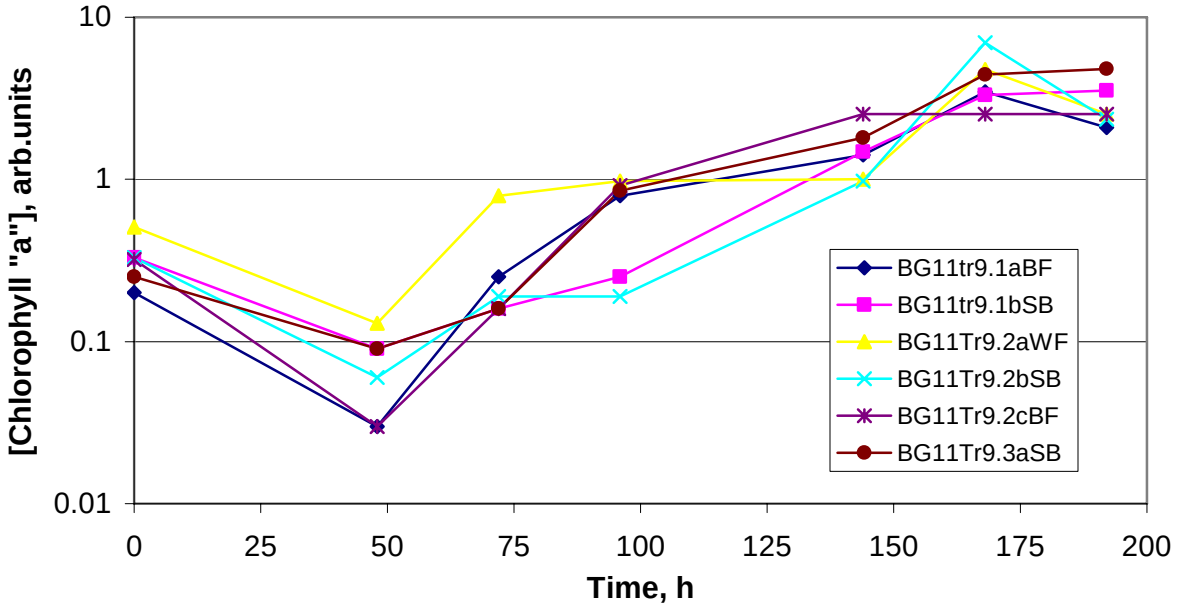

Fig. 11. Growth of isolates from Rabbit Creek area in BG-11 medium supplemented with 5 mM $NaHCO_3$ and aerated with 5% CO_2 in air.

Aeration of the cultures occurred at 48 hours after inoculation, explaining the decrease of chlorophyll concentration during first 48 hours. Aeration of the cultures led to the stimulation of growth. The exponential phase occurred from 50 to 150 hours approximately, as shown in Figure 11. Macroscopic *in situ* observation of bioreactor tubes with cyanobacterial cultures suggested that the growth rate of some cultures did not appear logarithmic in character because of significant adhesion to glass surfaces of the tubes.

Figure 12 shows the change in solution pH as a function of time due to carbon assimilation. The beginning of the exponential growth phase co-occurred with the relative stabilization of the pH

in the growth media. It appears a balance between the rate of photosynthetic fixation of CO_2/HCO_3^- and the rate of CO_2 supply develops. It is highly likely that balancing growth and pH changes in this way will be important in any future utilization of this technology.

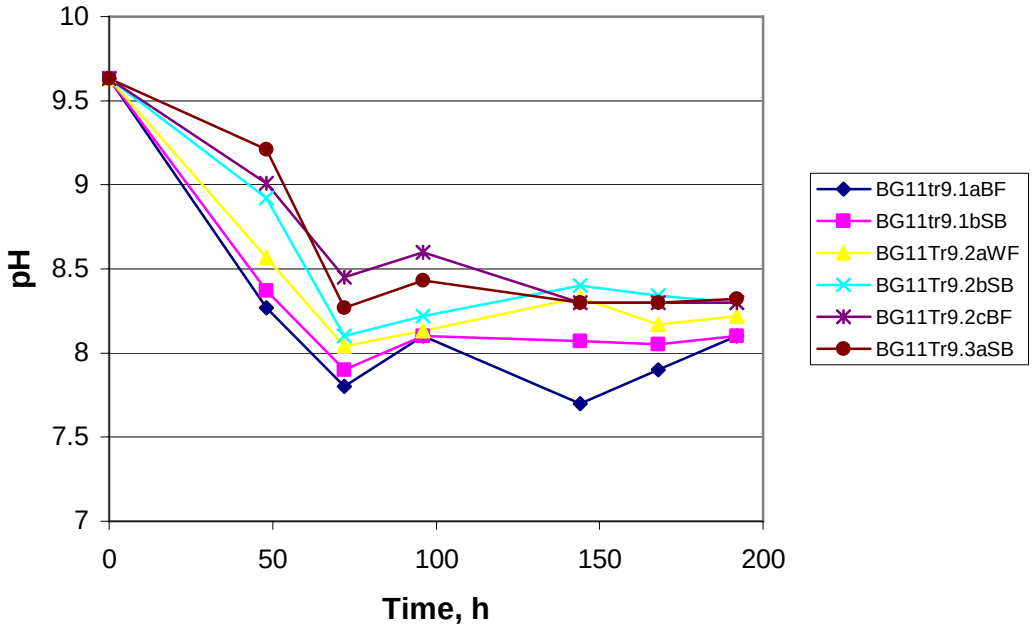

Fig. 12. pH dynamics in BG-11 medium, supplemented with 5 mM $NaHCO_3$ and aerated with 5% CO_2 in air during cultivation of isolates from Rabbit Creek area.

The growth of another group of isolates using the original media of their isolation is illustrated in Figure 13. The data indicate that cyanobacterial biomass increased up to 400 times original chlorophyll "a" units during five days of incubation. The average doubling time of this group of isolates approached 10 hours in the logarithmic phase of growth. Please note, however, that media was aerated simultaneously with the inoculation of cultures.

In the late log phase, cultures began to cause medium pH to rise. It is possible that at this time the rate of CO_2 supply was less than its consumption rate by cyanobacteria. We may speculate, therefore, that 5% CO_2 in air is not an upper concentration limit for the pilot plant cultivation of these isolates from Yellowstone National Park.

The doubling time of isolate s.c.1.2(3) was also measured and the results are shown in Figure 14. The culture was grown in BG-11 medium supplemented with 30 mM HEPES. Initial medium pH was 7.85. The medium was aerated with 5% CO_2 in air. The data suggest that the doubling time for s.c.1.2(3) isolate was about 7- 8 hours during exponential phase. The increase in doubling time of this organism during late logarithmic phase suggests that there were limiting factors, i.e. light and CO_2. This result supports the contention that thermophilic cyanobacteria have significant advantages as agents for practical photosynthetic CO_2 mitigation over their mesophilic forms.

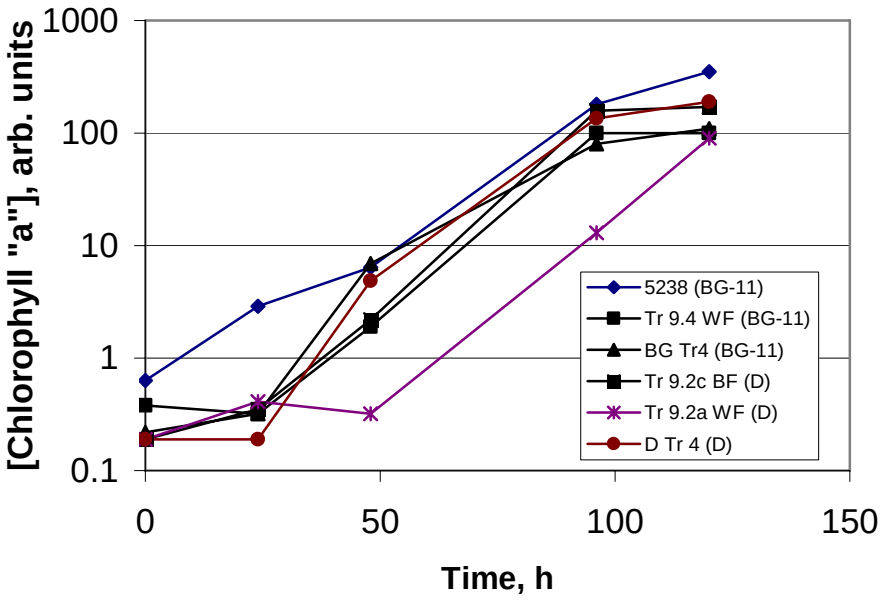

Fig. 13. Growth of isolates from Rabbit Creek area in BG-11 medium supplemented with 5mM $NaHCO_3$ and aerated with 5% CO_2 in air.

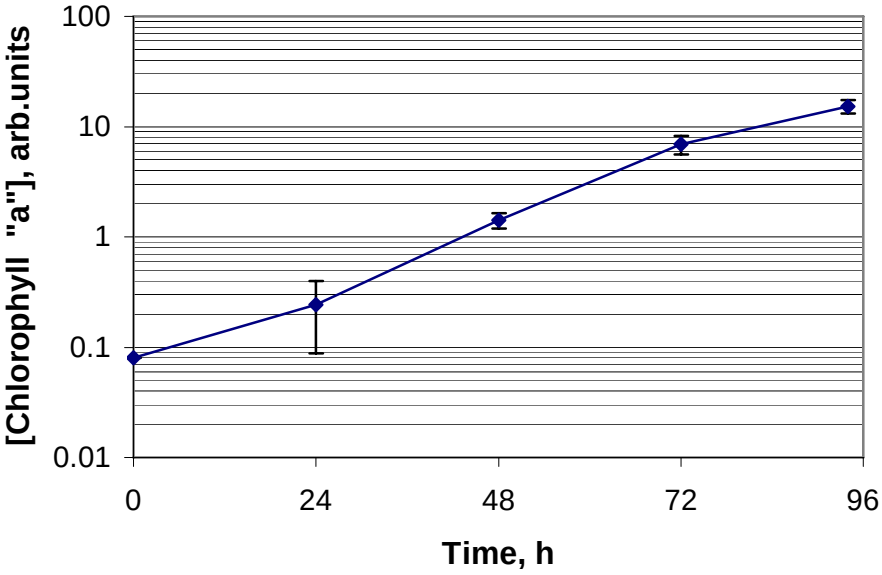

Fig. 14. Growth of s.c.1.2(3) isolate in BG-11 medium supplemented with 30 mM HEPES and aerated with 5% CO_2 in air. Doubling time was about 7.5 hours.

Figure 15 shows that the growth of s.c.1.2(3) isolate proceeds within a pH range of 7.5 – 7.9. (The pH of the environment where this culture was isolated was 7.6). CO_2 consumption by cyanobacteria during logarithmic phase exceeded the rate of CO_2 supply (10-15 mL/min), because alkalinization of growth medium was seen.

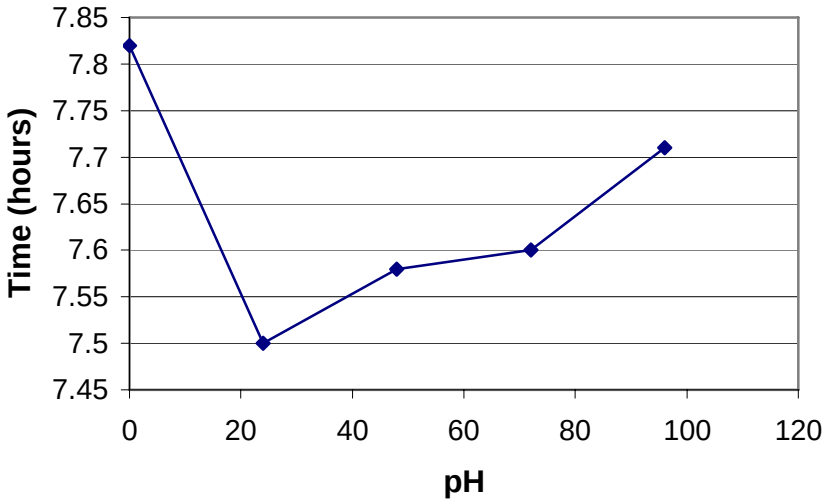

Fig. 15. pH dynamics during cultivation of s.c.1.2(3) isolate in BG-11 medium + 30 mM HEPES and aerated with 5% CO_2 in air.

The effect of very high CO_2 concentration is shown in Figure 16, which illustrates the growth of s.c.1.2(6) isolate in BG-11 buffered with 30 mM HEPES (initial pH 7.3) aerated with 15% CO_2 in air. The data indicates that 15% CO_2 does not inhibit the growth of s.c.1.2(6) isolate. In fact, the doubling time of this isolate was about 7.5 hours between 24 and 48 hours of cultivation, which is the shortest doubling time for any recorded thermophilic cyanobacterium.

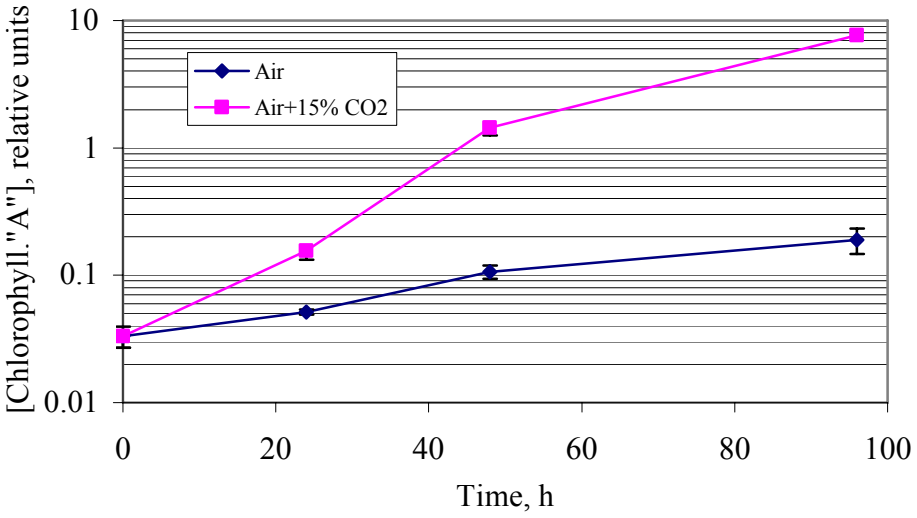

Fig. 16. Growth dynamics of s.c.1.2(6) isolate in buffered BG-11 medium aerated with different gas mixtures. The average doubling time between 24 and 96 hours was about 7.5 hours.

The experiment was repeated, this time with 5% CO_2 at the light level used for the previous experiment with 15% CO_2. Figure 17 reflects the result of this experiment. The growth curve of the isolate s.c.1.2(6) shows that doubling time of this isolate in neutral BG-11 medium aerated

with 5% CO_2 was about 7.5 hours for the period between 24 and 48 hours. This is the same doubling time that was found for this isolate for the period between 24 and 48 hours with 15% CO_2 (Fig.16).

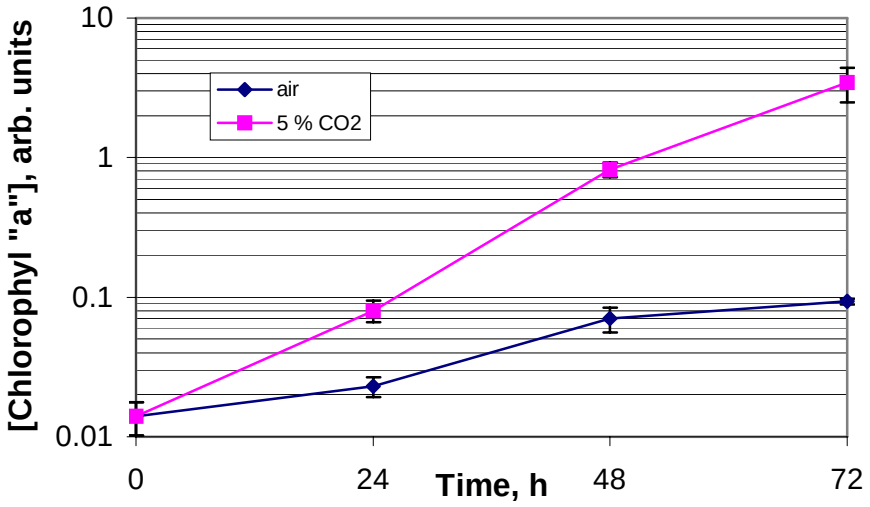

Fig. 17. Growth of s.c.1.2(6) isolate in buffered BG-11 medium aerated with 5% CO_2 in air. Between 24 and 96 hours was about 7.5 hours. The average doubling time in air alone was about 30 hours.

Since we were unable to measure dissolved CO_2, the exact concentration of CO_2 in liquid medium was different for different amounts of CO_2 in air. It is possible that the increase in CO_2 concentration in the gas phase did not affect significantly the level of dissolved CO_2 in the medium because of the high temperature (55^{o}C). As a result we observed neither repression nor stimulation of cyanobacterial growth when medium was aerated with 15% CO_2. It appears that the presence of CO_2 in the gas mixture stimulated growth of the cyanobacterium compared with just compressed air without CO_2.

1.1.9.2 Light effects: Growth of s.c.1.2(2) isolate with respect to illumination. An experiment to measure the effect of light on growth rate was carried out in the glass fermenter using 12 tubes for cultivation in BG-11 medium supplemented with 30 mM HEPES and aerated with 5% CO_2 in air. Gas flow was 10 mL/min for each tube. The tubes were separated into four series. The first three tubes were uncoated. The second, third and fourth series of tubes were consequently covered with 1, 2 and 3 layers of neutral gray window screening as shown in Figure 18. Integrated levels of the illumination of tubes are shown in Table 2.

Fig. 18. General view of the photoreactor with tubes coated with different screening mesh.

Table 2. Illumination levels.

The number of mesh layers	Integrated illumination
0	48 μE/m^2/sec
1	29 μE/m^2/sec
2	17 μE/m^2/sec
3	12 μE/m^2/sec

Data in Figure 19 suggests that doubling time of s.c.1.2(2) isolate was about 8 hours under integrated illumination level 48 μE/m^2/sec. Note that decreasing the illumination level below 48 μE/m^2/sec led to an increase in doubling time of this isolate as shown in Figure 20. It is evident that an illumination level of 50μE/m^2/sec does not saturate the system. Further, the doubling time of about 7.5 hours was affected when the illumination was approximately 170 μE .m^{-2}. sec^{-1}. Lower levels of illumination led to a decrease in cyanobacterial growth rate.

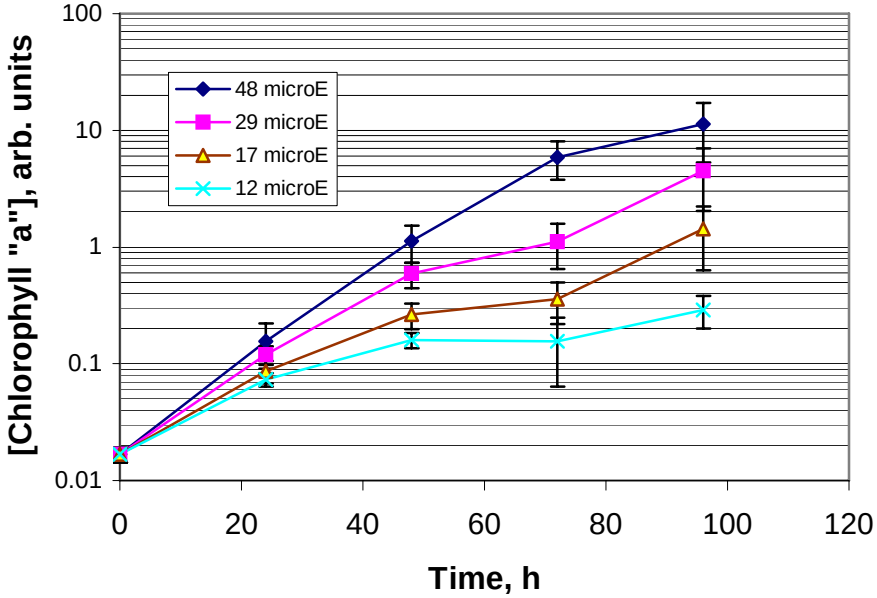

Fig. 19. Growth dependence of s.c.1.2(2) isolate on the level of illumination.

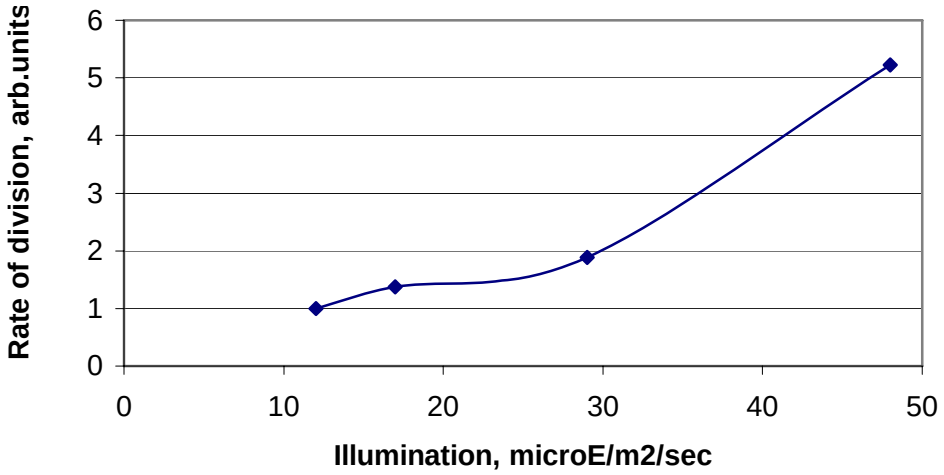

Fig. 20. Dependence of s.c.1.2(2) division rate on illumination level.

Our macroscopical and microscopical observations suggest that the culture of this isolate undergoes significant morphological changes after 60-70 hours of incubation in the batch culture mode. The culture begins to clump, which leads to the decrease of effective illumination of the culture because of a self-shading phenomenon. In addition, it is possible that this clumping of cells may reflect a decrease of combined nitrogen in the medium or medium alkalinization.

1.1.10 Tap water

Since the use of distilled water in a practical bioreactor may be precluded because of cost, even at the pilot-plant stage, experiments were performed to measure growth in BG-11 medium prepared with tap water. These experiments were carried out without aeration with 5% CO_2 in air. As shown in Figure 21, nearly all isolates (D Tr2WF, D Tr 9.2a WF, D Tr 9.2c BF, and D Tr4) grew well under the described conditions. It is important to note that tap water in Bozeman, MT, has a slightly alkaline pH and that the calcium concentration in this water is higher than was found in the medium prepared with distilled water. Note that Figure 22 shows that a buffer system $NaHCO_3/CO_2$ keeps the pH of cultures at a moderately alkaline level, even if the medium was prepared with tap water.

Because doubling time of cyanobacterial isolates cultivated in BG-11 medium prepared with tap water was longer than doubling time observed during incubation a medium prepared with distilled water, we conclude that this medium is less appropriate for the cultivation of cyanobacteria in the laboratory. However, this deficiency might be of lower importance at the pilot–plant stage because of the financial saving based on the use of tap water.

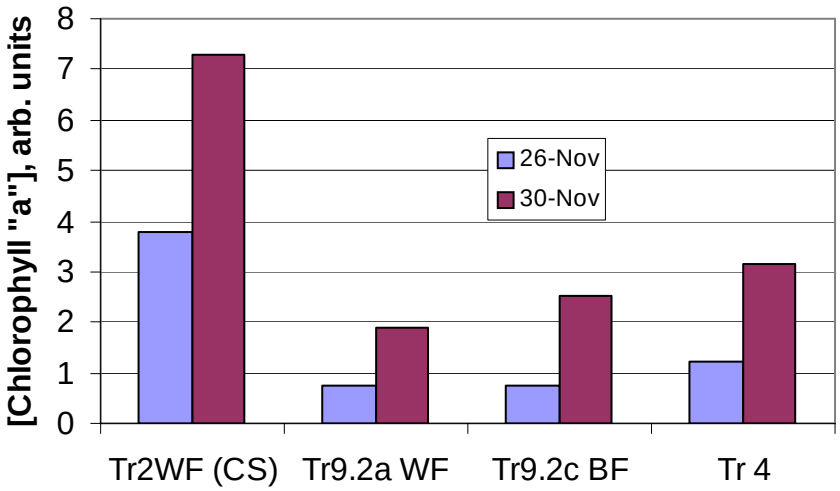

Fig. 21. Growth of four cultures (4 days) in BG-11 medium prepared with tap water.

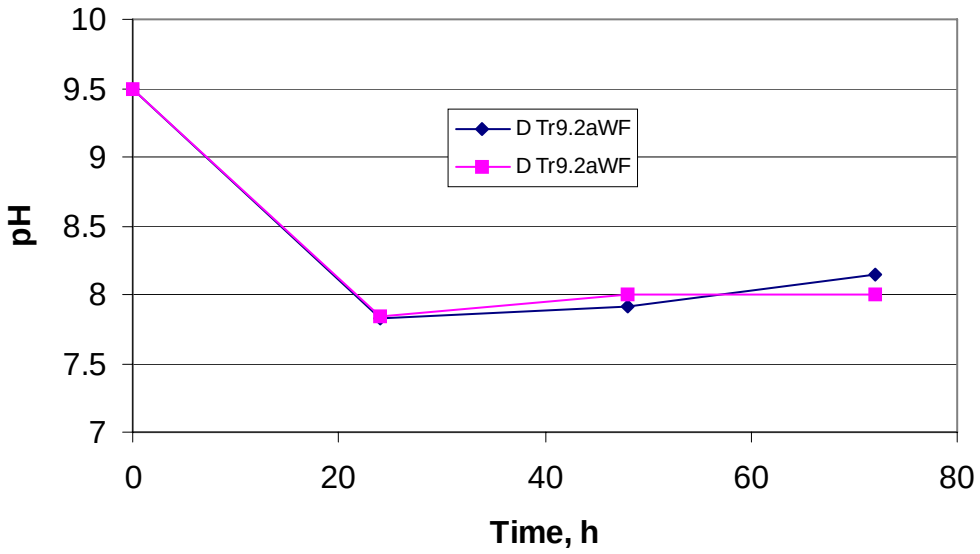

Fig. 22. pH dynamics during growth of Tr9.4WF isolate (in duplicate) in BG-11 medium prepared with tap water, supplemented with 5 mM of $NaHCO_3$ and aerated with 5% CO_2 in air.

1.1.11 The effect of iron on the growth

In next experiment, the importance of complex iron, which is normally included in BG-11 medium for the growth of thermophilic cyanobacterial isolates, was examined. Data shown in Figure 23 shows that added iron (0.04 mM) appears to be important for the growth of this cyanobacterial isolate, even in a medium prepared with Bozeman tap water, which contains 0.04 ppm iron. The growth rate is significantly lower without the iron.

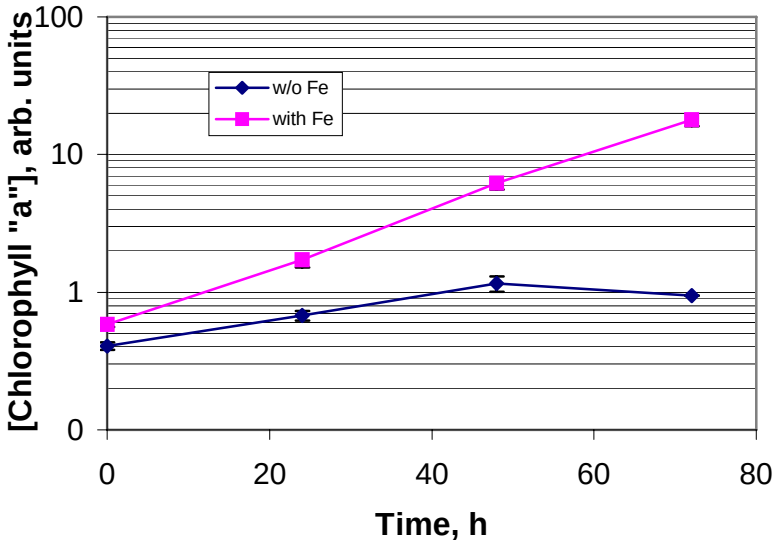

Fig. 23. Growth of the isolate D Tr 9.2c BF in BG-11 media prepared with tap water without and with added iron (0.04 mM).

The next test of the effect of iron used isolate 5.2 s. c.1 from the LaDuke Hot Spring in the Greater Yellowstone Basin. This spring is important because it has a concentration of iron as high as 0.44 ppm. This isolate and its cyanobacterial co-residents generate obvious cyanobacterial mats. An elevated resistance to iron might be very important for this project, because plant gases may have elevated amounts of iron. For these tests, ferric chloride was autoclaved twice before the inoculation of cyanobacteria into the experimental medium. The data, shown in Figure 24, shows that iron additions stimulated rather than inhibited the growth of 5.2. s.c.1 isolate.

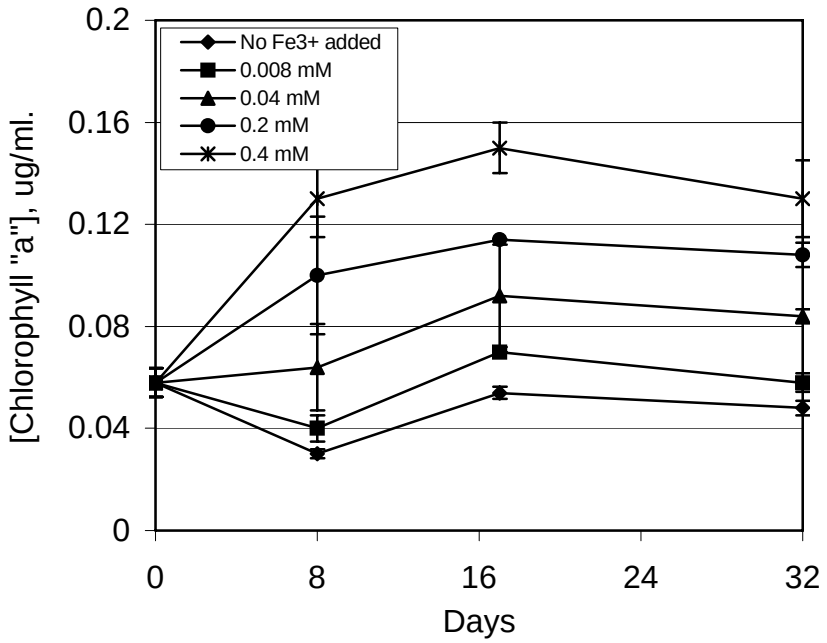

Fig. 24. Effect of Fe^{3+} concentration on the growth of 5.2 s.c.1 isolate.

1.1.12 Effects of calcium on cyanobacterial growth

The effect of Ca^{2+} on cyanobacterial adhesion was studied using a number of microscope cover slips (18mm) cleaned with Micro detergent – a treatment that has been shown to produce a very hydrophilic surface. Cover slips were placed in 10 mL beakers. Identical cell suspensions of cyanobacteria in media of differing Ca^{2+} concentration were added. The slips were covered with Parafilm to reduce evaporation and exposed to light for 4 hours. Then the cover slips with attached cyanobacterial cells were removed from the beakers. The glass substrata were dipped in fresh media (x 3) to remove unattached cells. Their lower surfaces were wiped with tissue to remove cells. They were then immersed in methanol to extract Chlorophyll "a" from the attached cells. Chlorophyll "a" was then determined fluorometrically. The results are represented in Figure 25. The adhesion of cyanobacteria to a glass surface depended on Ca^{2+}.

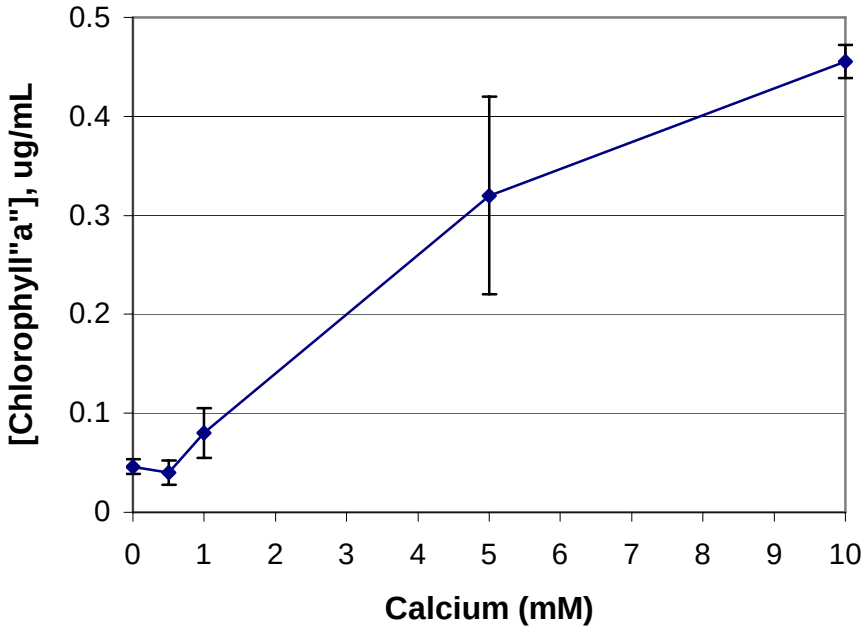

Fig. 25. Effect of Ca^{2+} concentration on the adhesion of isolate s.c.1.2(2) to a glass surface.

Chlorogloeopsis sp. was grown in the fermenter with all tubes filled with BG-11 medium, with 30 mM HEPES. The initial pH in the control tubes was 8.1 and in tubes with $CaCl_2$ it was 8.0. All the tubes were aerated with 5% CO_2 in air. We measured chlorophyll concentration and pH daily in all tubes. An addition of 10 mM of calcium stimulated further cell adhesion to walls of the bioreactor tubes as well as the generation of flocs of cyanobacterial cells.

The data, shown in Figure 26, suggest that calcium addition has a stimulating effect on the doubling of the s.c.1.2(2) culture. Figure 27 shows that calcium addition slowed down slightly the alkalinization of the growth medium.

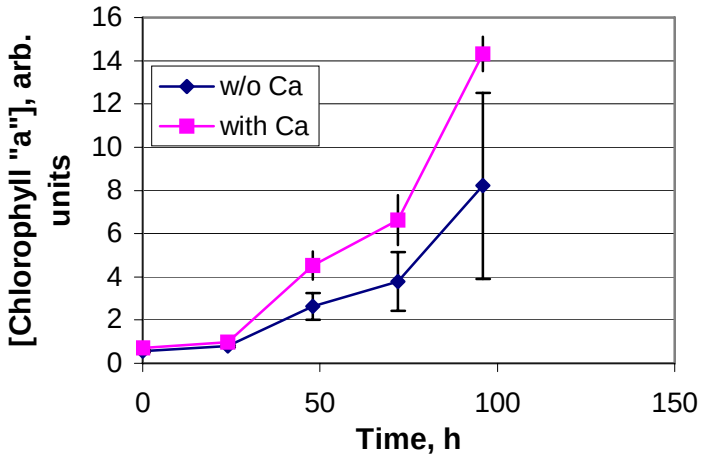

Fig. 26. Effect of Ca^{2+} on the growth of s.c.1.2(2) isolate in BG-11 medium with 30 mM HEPES and aerated with 5% CO_2 in air ("with Ca" refers to added 10mM of Ca).

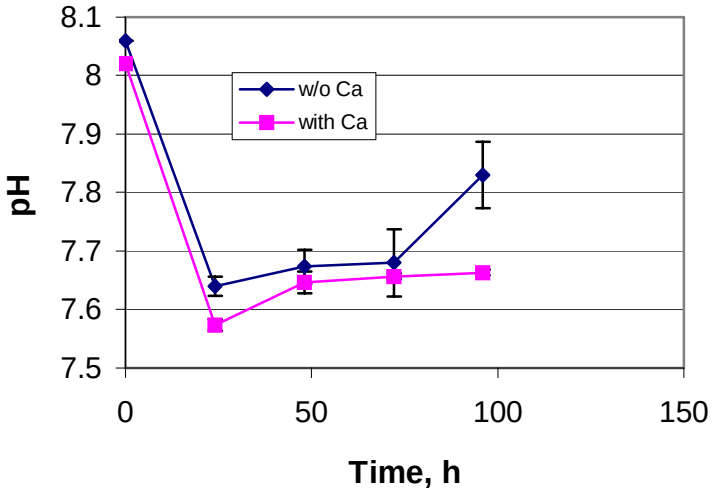

Fig. 27. Effect of Ca^{2+} on pH dynamics during growth of isolate s.c.1.2(2) in BG-11 medium, supplemented with 30 mM HEPES and 5% CO_2 in air.

The effect of calcium addition on the adhesion of s.c.1.2(2) isolate to Omnisil is shown in Figures 28 and 29. The coupons of this substratum were washed and autoclaved in BG-11 medium with 30 mM HEPES at a pH above 8. Early experiments had shown that acid treatment of Omnisil by the manufacturer tended to reduce the pH of the medium to unacceptably low levels. Coupons were placed in tubes with the same medium, but three tubes were filled with BG-11 + 30 mM HEPES + 10 mM $CaCl_2$. Despite the fact that the inoculum was low (in terms of cell number) colonization of edges of coupons was observed by the next day. Omnisil coupon edges were colonized more significantly than the central areas of these coupons. Figure 29 shows the general view of Omnisil coupons on fourth day of incubation. Notice that the coupons were colonized very well and that planktonic growth of isolate s.c.1.2(2) was not observed.

Fig. 28. Colonization of coupon edges by cyanobacteria**.**

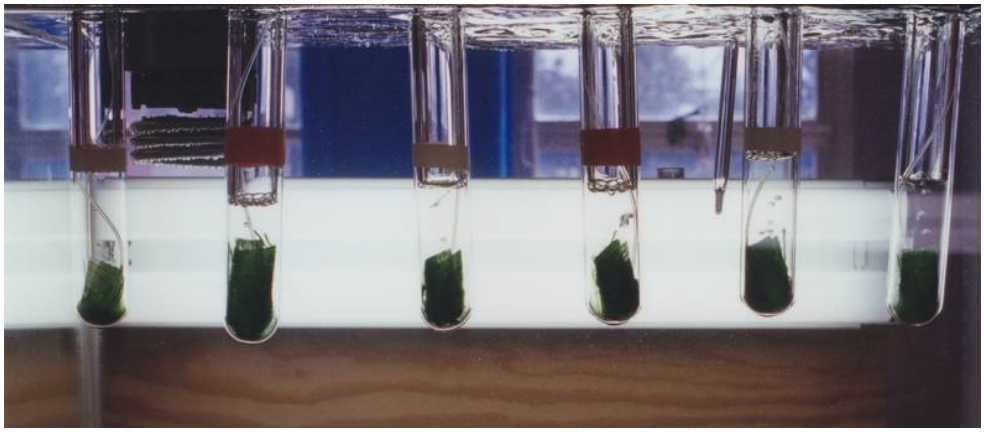

Fig. 29. General view of Omnisil coupons on the fourth day of their incubation.

Coupon # 1 (without calcium) and Coupon # 6 (with added calcium) were removed and rinsed three times in fresh BG-11 medium with 30 mM HEPES. Their images, shown in Figure 30, indicate that calcium stimulated the adhesion of cyanobacterial cells to Omnisil.

Fig. 30. Omnisil coupons are shown untreated (left) and treated with Ca^{2+} (right).

The surfaces of coupons # 1 and 6 were studied with help of scanning electron microscopy. Small squares of colonized coupons (approximately 4x4 mm) were cut and coated with gold. Figure 31 shows the growth without added calcium and Figure 32 is the image with added calcium. A comparison of the images suggests that the biofilm generated by isolate s.c.1.2(2) on an Omnisil surface in BG-11 medium supplemented with 10 mM of $CaCl_2$ is thicker and denser than that found without added Ca^{2+}.

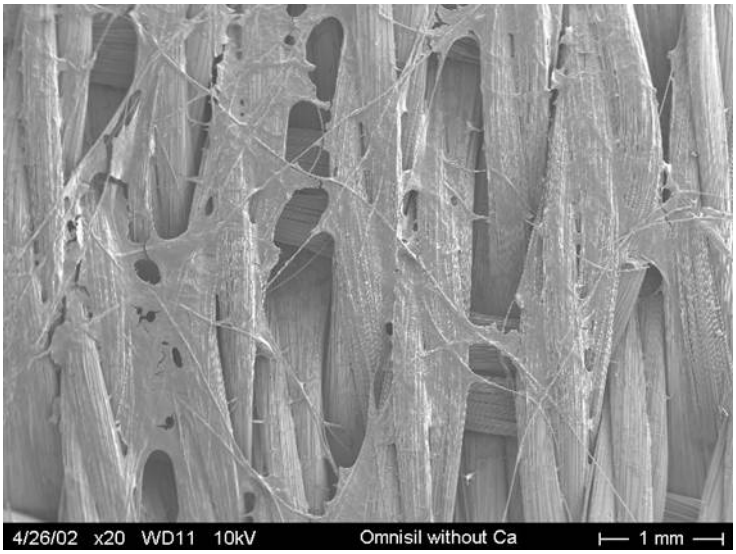

Fig. 31. Colonization of Omnisil by s.c.1.2(2) without added calcium.

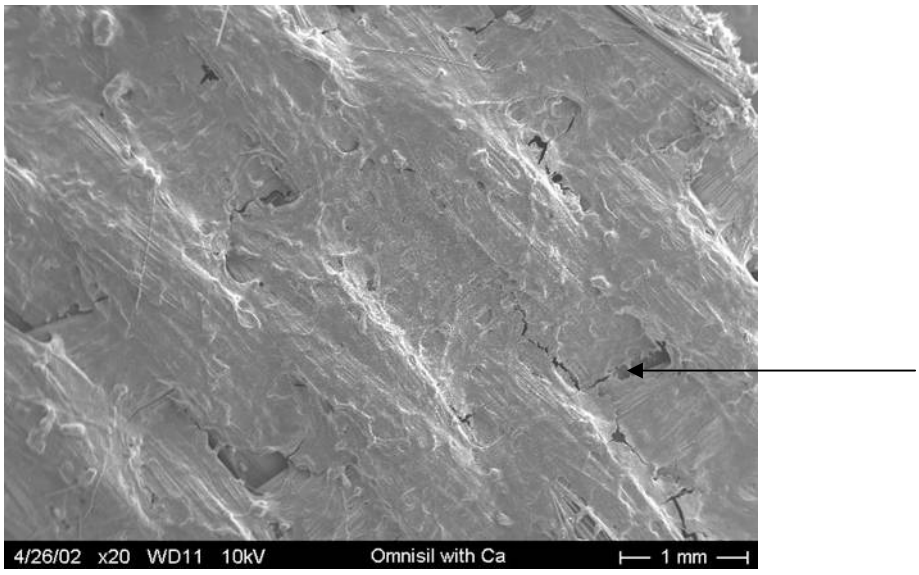

Fig. 32. Colonization of Omnisil by s.c.1.2(2) with added calcium
Arrow points to the surface irregularity of the biofilm surface.

The fibers of Omnisil are not visible in Figure 32, although they are quite evident in Figure 31 when the isolate was incubated without additional Ca^{2+}. Further magnification of the samples

(6400x shown in Figure 33) confirmed that adding calcium to the medium increased the density of the biofilm generated by isolate s.c.1.2(2).

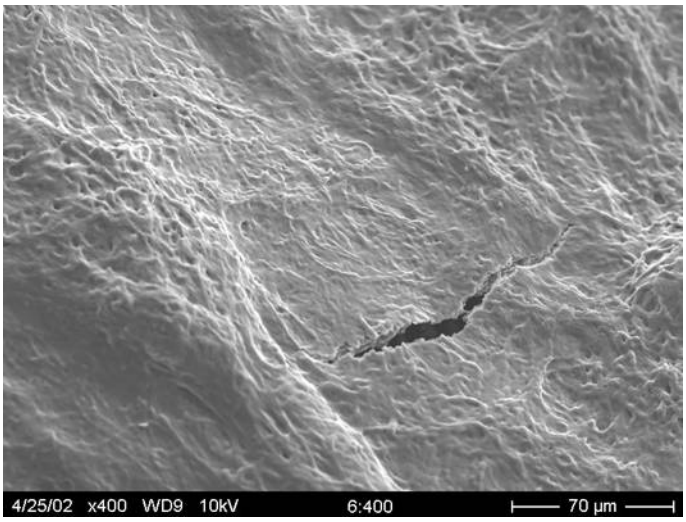

Fig. 33. Higher resolution SEM image of extracellular polymeric substance (EPS) of the cells.

Figure 34 shows one of typical irregularities in the biofilm surface when calcium was added. It is possible that the surface irregularities are the result of cell aggregation followed by subsequent growth of the cells stimulated by the calcium.

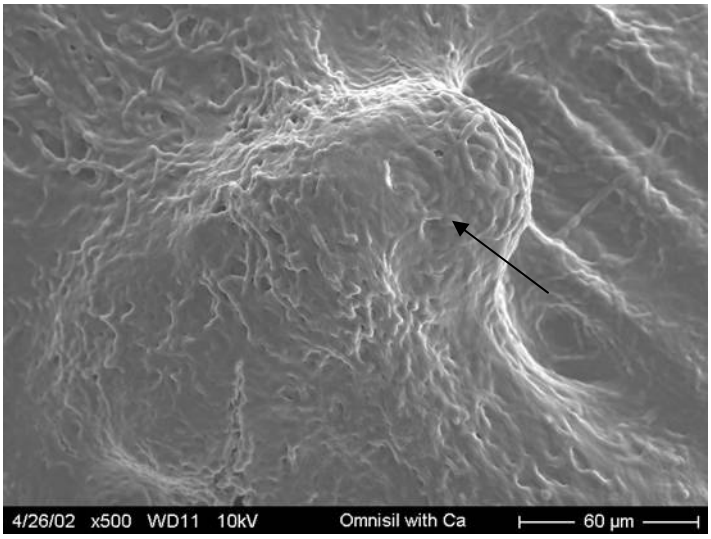

Fig. 34. A surface irregularity within s.c.1.2(2) biofilm induced by the addition of Ca^{2+}.

1.1.13 pH effects on the morphology of Chlorogloeopsis sp.

Macroscopic and microscopic observations suggest that this isolate undergoes morphological changes after 60-70 hours of incubation. The culture begins to clump, perhaps leading to a decrease in effective illumination at the cellular level. It is also possible that the clumping of

cells may reflect a decrease in combined nitrogen in the medium or a medium alkalinization. Because of this, we studied the effect of medium pH on the morphology of *Chlorogloeopsis* sp. isolates s.c.1.2(2) and (6). Our observations showed that non-starved *Chlorogloeopsis* sp. had chain-like shaped trichomes under neutral conditions, as shown in Figure 35. At this time, *Chlorogloeopsis* sp. cells incubated in alkaline medium had atypical shapes, i.e., they were tetrads, as shown in Figure 36.

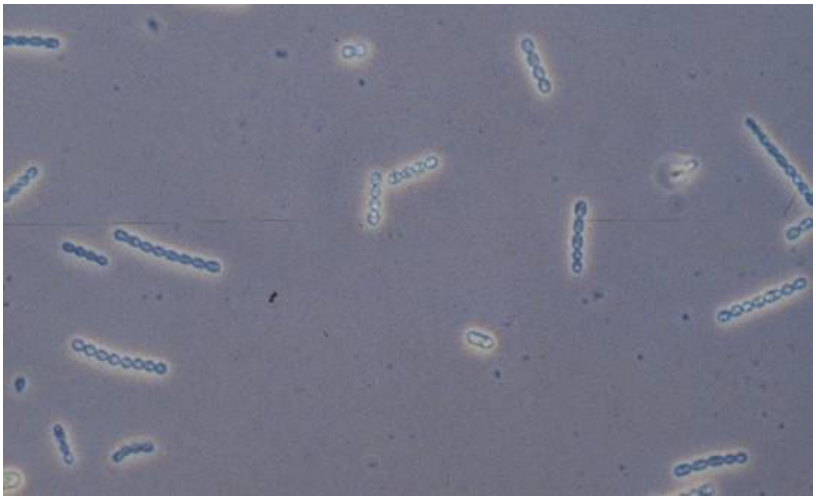

Fig. 35. Morphology of *Chlorogloeopsis* sp. cells incubated one month in BG-11 medium (pH 7) buffered with 30 mM HEPES.

Because both cultures were of the same age, we believe that the morphological changes are a result of stress induced by alkalinity, rather than N-insufficiency. Microscopical observation therefore may help to evaluate the stage and quality of *Chlorogloeopsis* sp. culture.

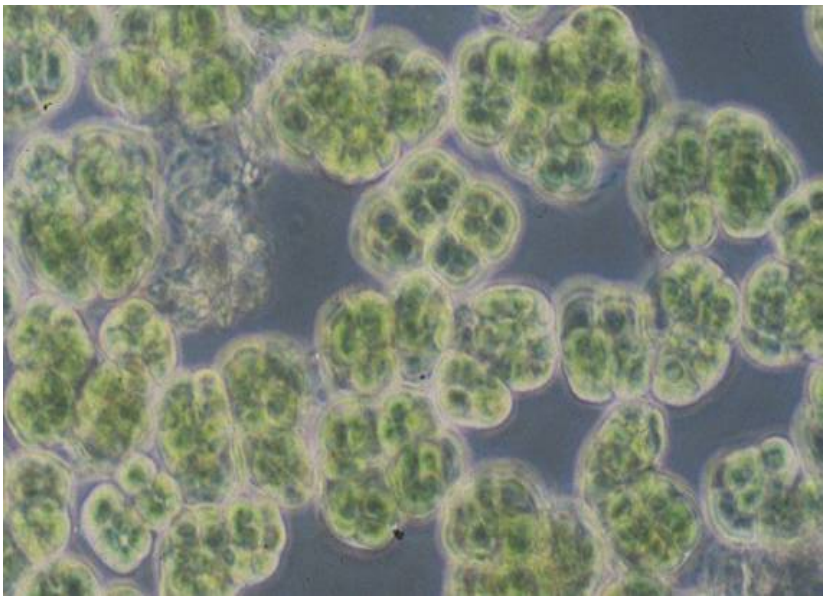

Fig. 36. Tetrad morphology of *Chlorogloeopsis* sp. incubated one month in alkaline (pH 9) BG-11 medium buffered with 30 mM (2-[N-cyclohexylamino]ethanesulfonic acid).

1.1.14 Genotyping

The following cyanobacterial isolates have been subjected to genotyping using 16-S RNA technology: 1.2 s.c. (2 and 6), 2.1 (III), 3.2.2 s.c. (1), 5.2 s.c.1, and 8.2.1 s.c. (10) using new primers recommended by Nubel *et al.* (1997). These primers are:

1. CYA106F CGG ACG GGT GAG TAA CGC GTG A
2. CYA359F GGG GAA TYT TCC GCA ATG GG
3. CYA781R(a) GAC TAC TGG GGT ATC TAA TCC CAT T
4. CYA781 (b) GAC TAC AGG GGT ATC TAA TCC CTT T

For the amplification of 16S rRNA from the isolates mentioned above, we used the primer CYA 106F and an equimolar mix of primers CYA781R (a) and (b). Using this mixture as a source of primers, we obtained PCR products from all isolates. These PCR products were purified with the help of a Quiagen Purification Kit. Purified PCR products were amplified in parallel using either CYA 106F or the mix of CYA781R (a) and (b).

The sequence of 16S rRNA for isolates s.c.1.2(2) and (6) were:

CGGTGGCTAAGACCGGATGTGCCGGGAGGTGAAAGGGAGACCGCCACAAGAGGAG
CTCGCGTCCGATTAGCTAGATGGTGGGGTAAAGGCCTACCATGGCGACGATCGGTA
GCTGGTCTGAGAGGACGAACAGCCCACACTGGGACTGAGACACGGCCCAGACTCCT
ACGGGAGGCAGCAGTGGGGAATTTTCCGCAATGGGCGAAAGCCTGACGGAGCAATA
CCGCGTGAGGGAGGAAGGCCCTTGGGTTGTAAACCTCTTTTCTCAGGGAAGAAGAA
ATGACGGTACCTGAGGAAAAAGCATCGGCTAACTCCGTGCCAGCAGCCGCGGTAAT
ACGGAGGATGCAAGCGTTATCCGGAATGATTGGGCGTAAAGGGTCCGTAGGTGGTG
ATGTATGTCTATTGTCAAAGGTTTCTGGCTTAACCAGAGACAGGCAGTAGAAACTGC
AAAACTAGAGTGCAGTCGGGGCAGGGGGAATTCCTGGTGTAGCGGTGAAATGCGTA
GAGTCAGGAAGAACACCGGGGCGAAAGCGCCCTGTAGGCT

The BLAST search showed a close alignment to the sequence of *Chlorogloeopsis* sp. PCC 7518 and *Chlorogloeopsis* sp. PCC 6718 with E value of 0.0. (These data can be found at [http://www.ncbi.nlm.nih.gov/blast/Blast.cgi#5814223]. Summarizing the morphological and molecular data we can conclude that isolate s.c.1.2(2) is a clone of *Chlorogloeopsis* sp.
The sequence for the isolate 3.2.2 s.c. 1 was:

CGGCTGCTAATACCCCATATGCCGCAAGGTGAAATCTTTTTTGGCCTGAG
GATGAGCTCGCGGTGGATTAGCTAGTTGGTGGGGTAATGGCCTACCAAGG
CAACGATCCATAGCTGGTCTGAGAGGATGATCAGCCACACTGGGACTGAA
GACACGGCCCAGACTCCTACGGGAGGCAGCAGTGGGGAATTTTCCGCAAT
GGGCGAAAGCCTGACGGAGCAAGACCGCGTGAGGGATGAAGGCCTTTGGGTTGTAA
ACCTCTTTTCTCAGGGAAGAACACAATGACGGTACCTGAGGAATAAGCCTCGGCTA
ACTCCGTGCCAGCAGCCGCGGTAAGACGGAGGAGGCAAGCGTTATCCGGAATTATT
GGGCGTAAAGCGTCCGCAGGTGGCTTTCCAAGTCTGCTGTCAAAACCCGAGGCTTAA
CCTCGGATCGGCGGTGGAAACTGGATCGCTAGAGTACGTCAGGGGTAGGGGGAATT

CCCGGTGTAGCGGTGAAATGCGTAGATATCGGGAAGAACACCAGCGACGAAAGGCC
CTACTGGGACG

These sequences were examined using the BLAST program and an excellent alignment to the thermophilic *Synechococcus* group was found. *Thermosynechococcus elongatus* and *Synechococcus elongatus* belong to this group [http://www.ncbi.nlm.nih.gov/blast/Blast.cgi]. The 16S rRNA sequences we obtained varied a little but this is not significant for the current stage of this project. The 16SrRNA sequences of six unialgal isolates were manually edited and compared to published sequences. Use of the BLAST search program revealed that isolates s.c.1.2(2) and (6) are completely identical and belong to the genus *Chlorogloeopsis* sp. It was also revealed that both isolates 3.2.2 s.c. 1 and 8.2.1 s.c. 10 belong to the genus *Synechococcus*, but to different lineages, i.e. to standard clones C1 and C9, respectively. This may explain their different physiological traits.

Because a partial sequence of 16S rRNA gene of the isolate 5.2 s.c.1 did not appear to be more than 93% identical to published cyanobacterial sequences, we carried out an entire sequence of this gene using the combination of different primers. We obtained a number of PCR products, which allowed us to arrive at a sequence of about 1350 nucleotides. The sequence of almost the entire16S r RNA subunit of the isolate 5.2 s.c.1 is unique. This may mean that we have found a representative of a putative new genus. The results of this work are represented in Table 3.

Table 3. Sequence data from unialgal cultures.

#	Name of isolate	Sequence	Genus
1	Isolate 1.2. s.c.6	CggtggctaagaccggatgtgccgggaggtgaaagggagaccgccacaagagGagc tcgcgtccgattagctagatggtggggtaaaggcctaccatggcgacgatcgGtagctgg tctgagaggacgaacagccacactgggactgagacacggcccagactCctacgggag gcagcagtggggaattttccgcaatgggcgaaagcctgacggagcAataccgcgtgag ggaggaaggcccttgggttgtaaacctcttttctcagggaagaaGaaatgacggtacctg aggaaaaagcatcggctaactccgtgccagcagccgcggTaatacggaggatgcaagc gttatccggaatgattgggcgtaaagggtccgtaggtggtgatgtatgtctAttgtcaaagg ttctggcttaaccagagacaggcagtagaaactgcaaaactagagtgcagtcggggcag ggggaattcctggtgtagcggtgaaatgcgtagagttcaggaagaacaccggtggcgaa agcgc	*Chlorogloeopsis* sp. (Rabbit Creek, YNP)
2	Isolate 8.2.1 s.c.10	GcaacccgcgtccttagttgccagcattcagttgggcactctggGgagactgccggtgac aagccggaggaaggtgcggatgacgTcaagtcagcatgccccttacgccctgggcgtc acacgtgctacaAtggccagcacaaagggtagccagccagcgatggtgagccaatCcc gcaaagttggtctcagttcagatcggagtctgcaactcgactCcgtgaaggcggaatcgct agtaatcgcaggtcagccatactgcggtgaatacgttcccgggccttgtacacaccgcccg tcacaccatgggagctggccacgcccgaagtcgttactccaaccgcaaggaggggagc gccgaaggcagggctggtgactggggtgaagtcgtaacaaggta	*Synechococcus* C9 type (Angel Terrace, Mammoth Hot Springs, YNP)

3	Isolate 3.2.2 s.c. 1	CggctgctaataccccatatgccgcaaggtgaaatctttttggccTgaggatgagctcgc ggtggattagctagttggtggggtaatggcCtaccaaggcaacgatccatagctggtctga gaggatgatcagccAcactgggactgaagacacggcccagactcctacgggaggcag CagtggggaattttccgcaatgggcgaaagcctgacggagcaagaCcgcgtgagggat gaaggcctttgggttgtaaacctcttttctcagggAagaacacaatgacggtacctgagga ataagcctcggctaactccgtgccagcagccgcggtaagacggaggaggcaagcgttat ccggaattattgggcgtaaagcgtccgcaggtggctttccaagctgctgtcaaaacccgag gcttaacctcggatcggcggtggaaactggacgctagagtacgtcaggggtaggggaa ttcccggtgtagcggtgaaatgcgtagatatcgggaagaacaccagcgacgaaaggccc tactgggacg	*Synechococcus* C1 type (Rabbit Creek, YNP)
4	Isolate 5.2 s.c.1	AcccgatatgccgagaggtgaaagtatttatagccttaaggggagctcgcGtctgattag ctagttggtagggtaagagcttaccaaggcgacgatcagtAgctggtctgagaggatgat cagccacactgggactgagacacggcccagActcctacgggaggcagcagtggggaa ttttccgcaatgggcgaaagcctGacggagcaataccgcgtgggggaggaaggctcttg ggttgtaaactcctTttctcagggaagaaaaaaatgacggtacctgaggaatcagcatcgg ctaActccgtgccagcagccgcggtaatacggaggatgcaagcgttatccggaAtcatt gggcgtaaagcgtccgcaggtggcacttcaagtctgctgtcaaaGgtcggggcttaactc cgaacaggcagtggaaactgaagcgctcgagtgcGgtaggggcagagggaattcctgg tgtagcggtgaaatgcgtagagatcaGgaagaacaccggtggcgaaagcgctctgctag gccgcaactgacactcaGggacgaaagctaggggagcgaatgggattagataccccag tagtcctagCtgtaaacgatggatactaggcgttgcttgtatcgacccaagcagtgccgTa gctaacgcgttaagtatcccgcctggggagtacgcacgcaagtgtgaaActcaaaggaa ttgacgggggcccgcacaagcggtggagtatgtggtttaAttcgatgcaacgcgaagaa ccttaccagggtttgacatgtccggaacccCgctgaaaggtgggggtgccttagggaacc ggaacacaggtggtgcatggCtgtcgtcagctcgtgtcgtgagatgttgggttaagtcccg caacgagcgCaaccctcgtttttagttgccagcattaagttgggcactctagaaagactGc cggtgacaaaccggaggaaggtggggatgacgtcaagtcagcatgcccCttacgctctg ggctacacacgtactacaatgctatggacaaagggcagcAagttagcgatgacaagcaa atcccataaaccatggctcagttcagatcgCaggctgcaactcgcctgcgtgaaggcgga atcgctagtaatcgccggtcAgccatacggcggtgaatacgttcccgggccttgtacaca ccgcccgtcaCaccatggaagcttggccacgcccgaagtcgttaccctaaccgcttgcg gaggggacgccgaaggcagg	*Chlorogloeopsis* sp. (Rabbit Creek, YNP)
5	Isolate 1.2. s.c. 2	CggtggctaagaccggatgtgccgggaggtgaaagggagaccgccacaagAggagc tcgcgtccgattagctagatggtggggtaaaggcctaccatggcGacgatcggtagctgg tctgagaggacgaacagccacactgggactgagaCacggcccagactcctacgggag gcagcagtggggaattttccgcaatggGcgaaagcctgacggagcaataccgcgtgag ggaggaaggcccttgggttGtaaacctcttttctcagggaagaagaaatgacggtacctg aggaaaaagcatcggctaactccgtgccagcagccgcggtaatacggaggatgcaagc Gttatccggaatgattgggcgtaaagggtccgtaggtggtgatgtatgtctattgtcaaagg ttctggcttaaccagagacaggcagtagaaactgcaaaactagagtgcagtcggggcag ggggaattcctggtgtagcggtgaaatgcgtagagttcaggaagaacaccggtggcgaa agcgccctgctaggct	
6	Isolate 2.1 (III)	cttccggtacggctaccttgttacgacttcaccccagtcaccagtcctaccttcggcgtcccc ctccgcgaacggttagggtaacgacttcgggcgtgacagcttccatggtgtgacgggcgg tgtgtacaaggcccgggaacgaattcctgcagtatgctgacctgcaattactagcgattccg acttcacgcaggcagtcgcagcctgcgatctgaactgagcccgagtttctgagatttgcttg	*Mastigocladus* sp. (Rabbit Creek, YNP)

		tattcgcatacttgctgccctttgtctcgagcattgtagtacgtgtgtagccaggacgtaagg ggcatgctgacttgacgtcatccccaccttcctccgtttgtcaccggcagtctccctagagtg cccacccgaagtgctggcaactagaacgagggttgcgctcgttgcgggacttaacccaac atctcacgacacgagctgacgacagccatgcaccacctgtgttctggctcccgaaggcac ctcagctttcaccgaagttccagacatgtcaagccctggtaaggttcttccgttgcatcgaatt aaaccacatactccaccgcttgtgcgggcccccgtaattcctttgagtttcacacttgcgtgc gtactccccaggcgggatacttaacgcgttagctacggcactgagagggtcgatactctca acgcctagtatccatcgtttacggctaggactactggggtatctaatcccattcgctccccta gctttcgtccctcagtgtcagttgcggcctagcagagcgctttcgccaccggtgttcttcctg atctctacgcatttcaccgctacaccaggaattccctctgccccgaacgcactctagtcgtgt agtttctactgcctttatcatgttaagcatgatgctttgacaatagacacacacaaccacctgc ggacgctttacgcccaatcattccggataacgcttgcatcctccgtattaccgcggctgctg gcacggagttagccgatgctgattcctcaagtaccgtcagaacttcttccttgagaaaagag gtttacaacccaagagccttcctccctcacgcggtattgctccgtcaggctttcgcccattgc ggaaaattccccactgctgcctcccgtaggagtctggaccgtgtctcagttccagtgtggct gatcatcctctcagaccagctactgatcgtcgccttggtagtcccttacaccaccaactagct aatcagacgcgagctcttcttcaggcrgcwagcctttcacctctcggcacatccggtattag catcggtttcccaatgttgtcccgaacctgaagctagattctcacgcgttactcacccgtccg ccactatgtagagacctagcattgctacgtctctacatcgttcgacttgcatgtgttaagcata ccgccagcgttcatc	

1.1.15 Motility of isolates

A stable culture of unicellular species 8.2.1 *Synechococcus* s.c. (10) from samples obtained from Angel Terrace (Mammoth Hot Springs) was isolated from an environment characterized with an elevated concentration of CO_2 and dissolved calcium. After isolating a working culture of *Synechococcus* sp., the culture was streaked on semi-solid (agarose 2.5%) BG-11 medium. After 2 months of incubation in a humid chamber, 10 clones of *Synechococcus* were chosen from the agarose surface and inoculated in liquid BG-11 medium (0.5 mL). After 1.5 months exposure, the inocula grew, although poorly. They were transferred to glass tubes with 1.5 mL of fresh BG-11 medium. Clone # 10 gave the best growth and this was transferred to a flask with fresh medium. Just because an organism is slow to grow on initial isolation does not obviate its utility in the CRF.

Motile ability of 8.2.1 *Synechococcus* s.c. (10) and 3.2.2 *Synechococcus* s.c. 6 was measured. The ability of cells to migrate is important in filamentous cyanobacteria, which have a motile phenotype, but coccoid cells are usually non-motile. However, Ramsing ***et al.*** showed that a thermophilic *Synechococcus* sp. that inhabited a natural microbial mat exhibited negative phototaxis. Cells on the screen/membrane that supports cyanobacterial growth in the CRF facility may experience both light and nutrient gradients. Photostimulation of cyanobacterial motility may promote even colonization of the support.

Unicellular isolates 8.2.1 *Synechococcus* s.c. (10) and 3.2.2 *Synechococcus* s.c. 1 are phototactic and are shown in Figures 37 and 38. Isolate 3.2.2 *Synechococcus* s.c. 1 currently consists of two populations: one population appears to be positive phototactic, and the second population appears negative phototactic to the same level of light (Figure 38). This implies that illumination

of the cell support in the CRF should be as uniform as possible and reasonable for cyanobacterial cells.

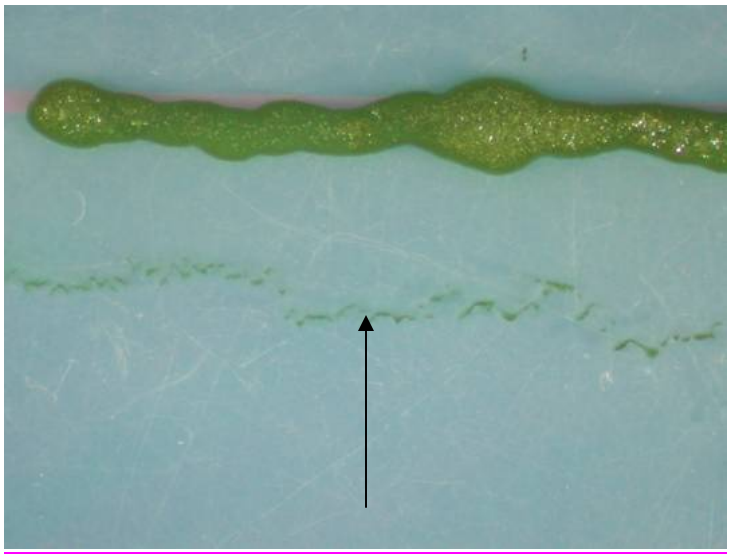

Fig. 37. The arrow points to the phototactic population of the isolate 8.2.1 *Synechococcus* s.c. (10). The arrow also shows the light direction.

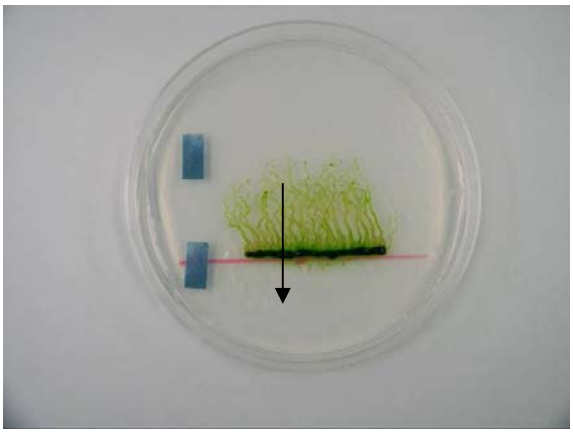

Fig. 38. The arrow points to the phototactic population of the isolate 3.2.2 *Synechococcus* s.c. (10). The arrow also shows the light direction.

1.1.16 Selection of acid resistant clones from 3.2.2 s.c.1

Analysis of growth data showed a pitfall in the cultivation of thermophilic cyanobacteria under elevated concentrations of CO_2. In the absence of a buffering agent, there is significant acidification of the growth medium by CO_2. A short-term proposal to overcome this problem is the use of buffers such as HEPES, to prevent medium acidification. This is unlikely to become a solution in practice because of the expense of this buffer. The ability of cyanobacteria to glide on a semisolid surface was utilized in an endeavor to select acid resistant clones.

Unicellular culture "3.2.2 s. c.1 Positive" was chosen for this experiment because it was motile and positively phototactic. In this context "positive" means that we have isolated the population with high rate of motility towards light from general culture of 3.2.2 s. c. 1. Furthermore, 3.2.2 s. c. 1 is a unicellular culture and there was a reasonable expectation that a clonal mutant from the culture 3.2.2 s.c.1 might be obtained more easily than from multicellular culture s.c.1.2(2).

Two types of Petri dishes were prepared: the first group of dishes was filled with semisolid BG-11 medium supplemented with 30 mM HEPES (pH 7.4). The second group of dishes was filled in two steps. First, we poured about 12 mL of BG-11 medium supplemented with 30 mM (2-[N-Morpholino]ethanesulfonic acid, MES, pH 4.0) into a Petri dish, which was positioned with a small angle to horizontal surface. When this medium had solidified, the Petri dish was positioned on horizontal surface and 15 mL of the medium with pH 7.4 was poured in the depression between solidified medium and dish wall. Approximately 20 µL of high-density "3.2.2 s.c.1 Positive" culture was inoculated onto the surface of both Petri dishes. They were wrapped with aluminum foil so they received light from one side only. Results are presented in Figures 39-41.

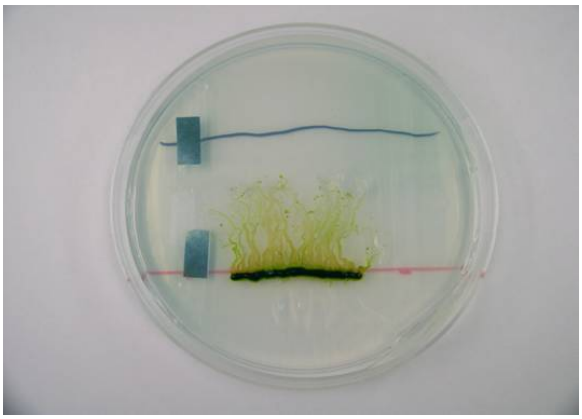

Fig. 39. General view of migrating population of "3.2.2 s.c.1 Positive" on semi-solid BG-11 medium with an acid gradient**.** Light gradient was perpendicular to red line on dish bottom.

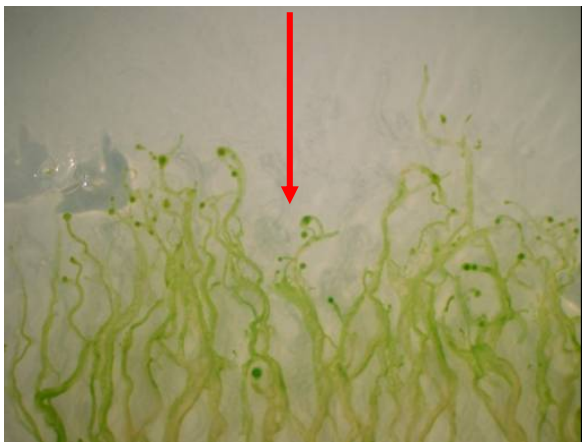

Fig. 40. Photomicrograph of leading edge of "3.2.2 s.c.1. Positive" migrating along semisolid BG-11 medium, pH 7.4, toward light. Red arrow indicates light direction.

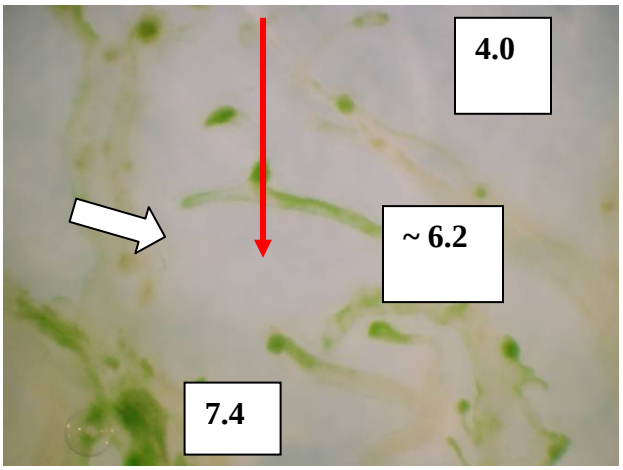

Fig. 41. Photomicrograph of leading edge of "3.2.2 s.c.1 Positive" migrating toward light along semi-solid BG-11 medium with a pH gradient (shown numerically).

As can be seen in Figures 39 and 40, microcolonies of "3.2.2 s.c.1 Positive" culture migrated mainly toward light along a light gradient when the medium pH was close to neutral. As can be seen in Figure 41, microcolonies approaching the area with lowest pH changed migration direction to one that was almost perpendicular to both light and acid gradient. Nonetheless, some microcolonies were able to generate "secondary" microcolonies with an enhanced ability to move toward the acidic area.

These microcolonies with elevated resistance to acidity have been isolated and inoculated in BG-11 at pH 6, providing a population of 3.2.2 s.c.1 that is resistant to pH 6.

Subtask 1.2 Design deep-penetration light delivery subsystem

The central problem to the successful implementation of a vertical substrate bioreactor is lighting. As shown in Figure 42, our approach was to bring and distribute light within the bioreactor using a solar photon (light) collector and a fiber optic distribution system.

In order to get light to the suspended membranes, the next-generation "illumination sheet" was developed consisting of 10 meters of side-emitting optical fiber sandwiched between two clear plexiglass sheets. The optical fiber was formed into a serpentine pattern before being mounted in a plexiglass frame, similar to that shown in Figure 43. A mirror, fixed to the end of the optical fiber, reflects light back toward the optical source. The reflecting mirror greatly improves the efficiency and intensity distribution of the illumination sheet. The illumination sheet emits light from both sides of the sheet.

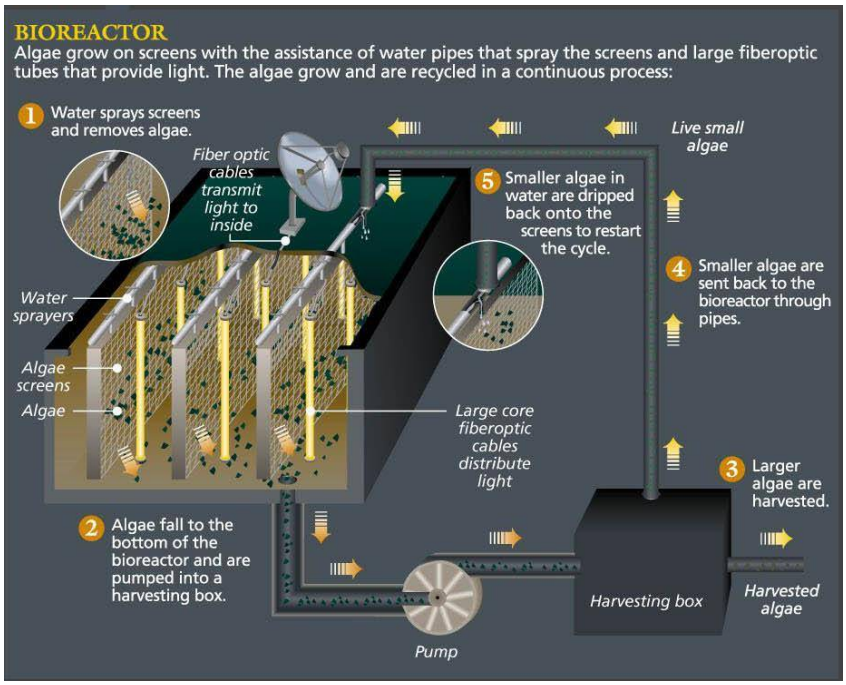

Fig 42. Schematic of the bioreactor system with light collection and delivery.

During construction of the original prototype illumination sheet, it was found that excessive losses, due to acute bends in the serpentine fiber pattern, resulted in an uneven illumination distribution. To avoid the uneven intensity distribution, experiments were performed to characterize the optical fiber loss as a function of bend radii. Given the ability to predict the optical loss in a fiber bend, the serpentine pattern was modified to maximize the amount of light reaching the far side of the illumination sheet.

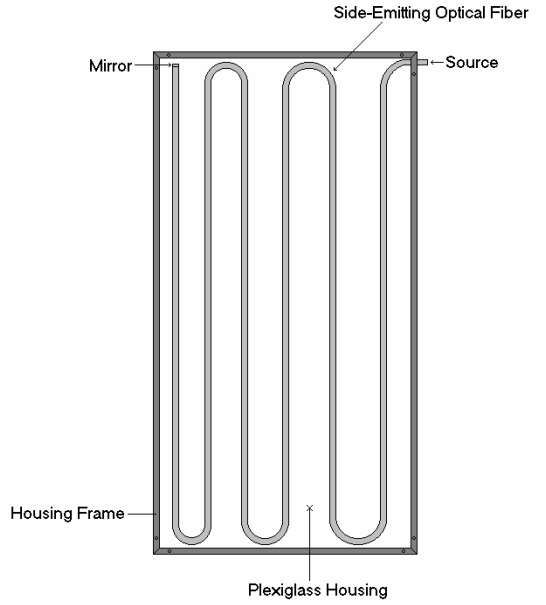

Fig. 43. Side-emitting fiber illumination sheet.

A solar collector, shown in Figure 44, was installed immediately above the bioreactor. The light reflects off the primary mirror onto a secondary mirror, which focuses the light on eight fiber optic cables. The cables are shown in Figure 45. To quantify the photon flux in the bioreactor, each of the light sheets was divided into a grid of 3x5 to give 15 readings for each. The sheets are marked A, B, C, D, E, F, G, and H (left to right) when seen from the growth tank side. Each sheet provided 2 sets of 15 readings for both surfaces. For simplicity we have used conventions A(L) and A(R) for each sheet which represent the left and right side of the sheet (again when looked at from the growth tank side). Designating the membranes 1, 2, 3 … etc., then #1 will receive light from A(R) and B(L). The locations of these panels in the bioreactor are shown in Figures 45 and 46. The readings for the respective panels are shown in Table 4.

Fig. 44. Solar collector installed above the bioreactor.

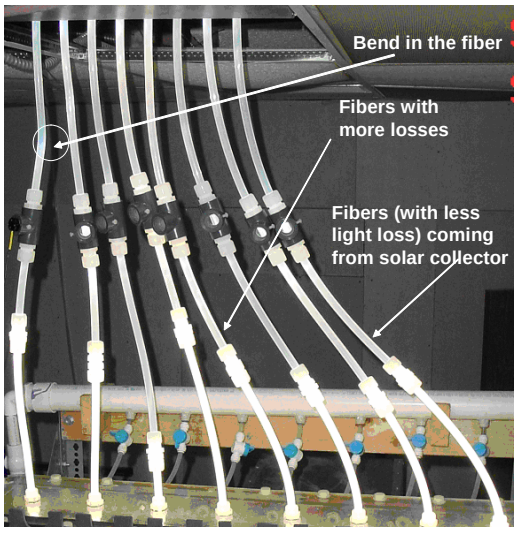

Fig. 45. Lighting panel notes and designations.

Fig. 46. Lighting sheets in bioreactor.

Table 4. Photon flux measurements (in μmols m^{-2} s^{-1}).

A(R)		
43.8	44.6	32.7
50.5	36.4	43.8
25.3	29.7	43.8
29.7	29.0	39.4
46.8	36.4	60.2
B(R)		
52.0	44.6	57.2
44.6	57.2	58.0
38.6	44.6	52.0
43.1	40.9	52.0
72.1	46.1	78.8
C(R)		
55.7	51.3	66.9
46.1	66.1	61.7
37.2	51.3	57.2
43.8	51.3	60.9
97.3	48.3	85.4
D(R)		
45.3	47.6	55.0
54.2	63.2	44.6
39.4	49.0	51.3
44.6	49.8	50.5
51.3	44.6	65.4
E(R)		
50.5	47.6	60.2
40.9	55.0	54.2
42.4	44.6	58.7
40.9	46.1	51.3
64.2	43.1	84.0
F(R)		
57.2	53.5	69.1
44.6	63.9	56.5
43.8	49.8	59.4
44.6	52.8	60.2
63.2	49.0	98.1
G(R)		
58.0	49.8	60.2
46.1	63.9	61.7
47.6	54.2	63.2
46.1	54.2	60.2
33.6	50.5	91.4

B(L)		
69.8	57.2	84.0
67.6	79.5	50.5
63.2	59.4	44.6
67.6	66.1	52.0
117.4	52.8	92.1
C(L)		
58.7	60.9	74.3
62.4	46.8	73.6
49.8	46.1	71.3
61.7	48.3	60.2
150.8	56.5	112.9
D(L)		
61.7	55.7	63.2
53.5	69.1	46.8
53.5	55.7	43.1
58.7	55.7	46.8
91.4	48.3	81.7
E(L)		
66.1	57.2	64.6
48.3	60.9	70.3
58.7	52.8	47.6
57.2	63.9	45.3
134.5	51.3	102.5
F(L)		
67.6	54.2	71.3
67.6	81.0	49.0
63.2	66.9	48.3
63.2	66.1	50.5
125.6	58.0	101.8
G(L)		
58.0	51.3	76.5
61.7	66.1	51.3
56.5	67.6	51.3
54.2	47.6	46.1
138.9	71.3	105.5
H(L)		
55.7	43.8	63.2
53.5	49.8	38.6
49.8	44.6	34.9
52.8	39.4	32.7
173.9	37.2	130.8

Table 5. Maximum, minimum, and average amount of flux delivered by light sheets.

	A(R)	B(L)	B(R)	C(L)	C(R)	D(L)	D(R)
MAX.	60.2	117.4	78.8	150.8	97.3	91.4	65.4
	50.5	92.1	72.1	112.9	85.4	81.7	63.2
	46.8	84.0	58.0	74.3	66.9	69.1	55.0
	44.6	79.5	57.2	73.6	66.1	63.2	54.2
	43.8	69.8	57.2	71.3	61.7	61.7	51.3
	43.8	67.6	52.0	62.4	60.9	58.7	51.3
	43.8	67.6	52.0	61.7	57.2	55.7	50.5
	39.4	66.1	52.0	60.9	55.7	55.7	49.8
	36.4	63.2	46.1	60.2	51.3	55.7	49.0
	36.4	59.4	44.6	58.7	51.3	53.5	47.6
	32.7	57.2	44.6	56.5	51.3	53.5	45.3
	29.7	52.8	44.6	49.8	48.3	48.3	44.6
	29.7	52.0	43.1	48.3	46.1	46.8	44.6
	29.0	50.5	40.9	46.8	43.8	46.8	44.6
MIN.	25.3	44.6	38.6	46.1	37.2	43.1	39.4
Sum	**592.2**	**1023.9**	**781.6**	**1034.3**	**880.5**	**884.9**	**755.6**
Avg.	39.5	68.3	52.1	69.0	58.7	59.0	50.4

	E(L)	E(R)	F(L)	F(R)	G(L)	G(R)	H(L)
MAX.	134.5	84.0	125.6	98.1	138.9	91.4	173.9
	102.5	64.2	101.8	69.1	105.5	73.6	130.8
	70.3	60.2	81.0	63.9	76.5	63.9	63.2
	66.1	58.7	71.3	63.2	71.3	63.2	55.7
	64.6	55.0	67.6	60.2	67.6	61.7	53.5
	63.9	54.2	67.6	59.4	66.1	60.2	52.8
	60.9	51.3	66.9	57.2	61.7	60.2	49.8
	58.7	50.5	66.1	56.5	58.0	58.0	49.8
	57.2	47.6	63.2	53.5	56.5	54.2	44.6
	57.2	46.1	63.2	52.8	54.2	54.2	43.8
	52.8	44.6	58.0	49.8	51.3	50.5	39.4
	51.3	43.1	54.2	49.0	51.3	49.8	38.6
	48.3	42.4	50.5	44.6	51.3	47.6	37.2
	47.6	40.9	49.0	44.6	47.6	46.1	34.9
MIN.	45.3	40.9	48.3	43.8	46.1	46.1	32.7
Sum	**981.3**	**783.5**	**1034.3**	**865.6**	**1003.8**	**880.5**	**900.5**
Avg.	65.4	52.2	69.0	57.7	66.9	58.7	60.0

Shown next (Figure 47a-h) below are the graphs corresponding to the data in Table 4. Please refer to Figure 45 to understand the position of light panels A-H.

A(R)

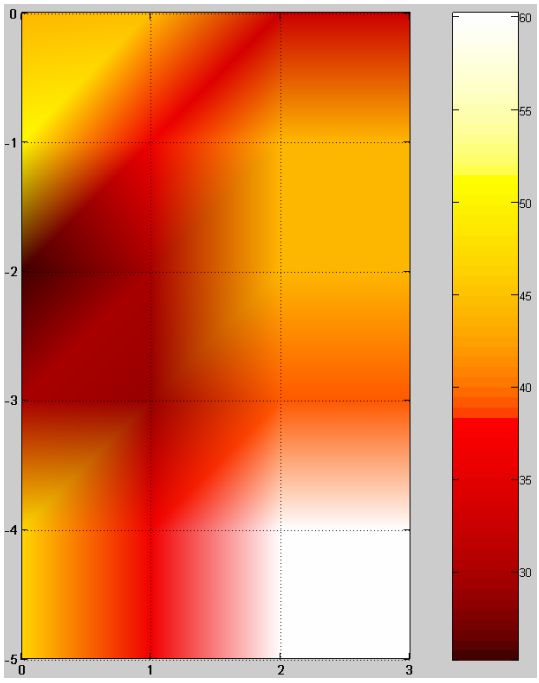
0
-1
-2
-3
-4
-5
0
1
2
3
60
55
50
45
40
35
30

B(L)

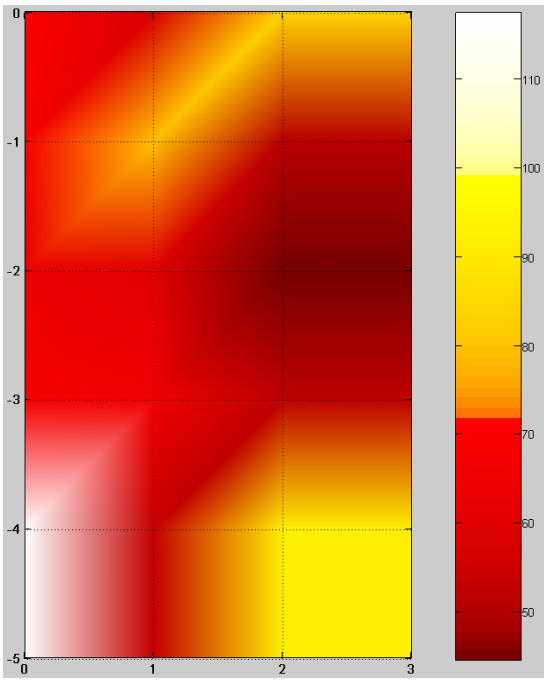
0
-1
-2
-3
-4
-5
0
1
2
3
110
100
90
80
70
60
50

B(R)

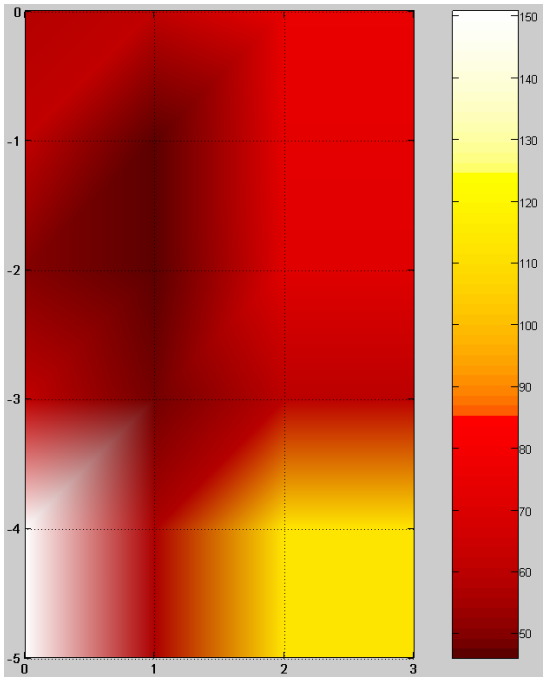
0
-1
-2
-3
-4
-5
0
1
2
3
150
140
130
120
110
100
90
80
70
60
50

C(L)

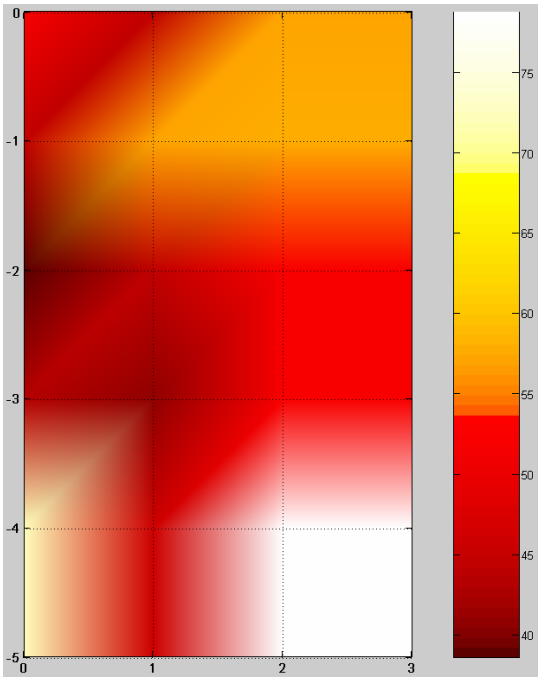
0
-1
-2
-3
-4
-5
0
1
2
3
75
70
65
60
55
50
45
40

C(R)

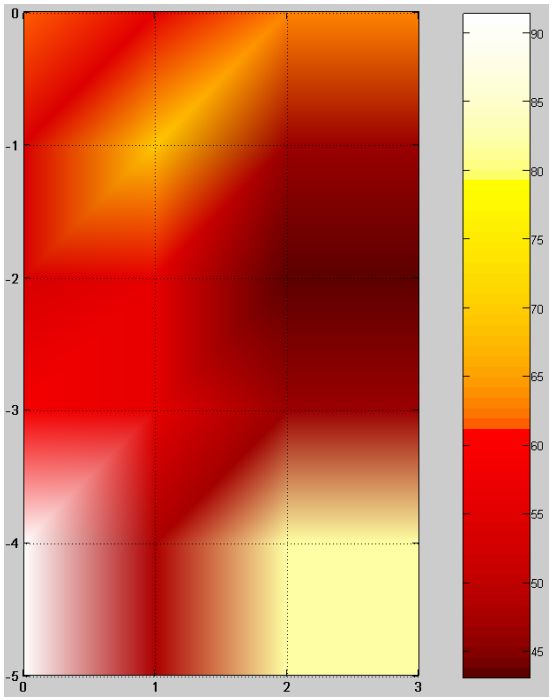
0
-1
-2
-3
-4
-5
0
1
2
3
90
85
80
75
70
65
60
55
50
45

D(L)

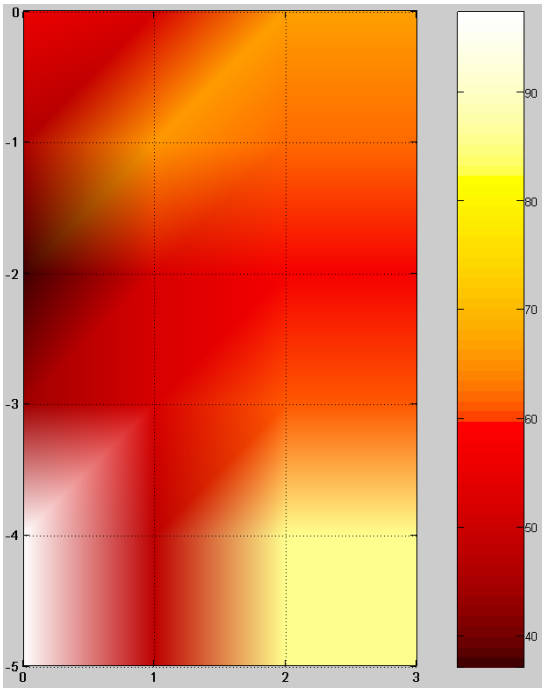
0
-1
-2
-3
-4
-5
0
1
2
3
90
80
70
60
50
40

D(R)

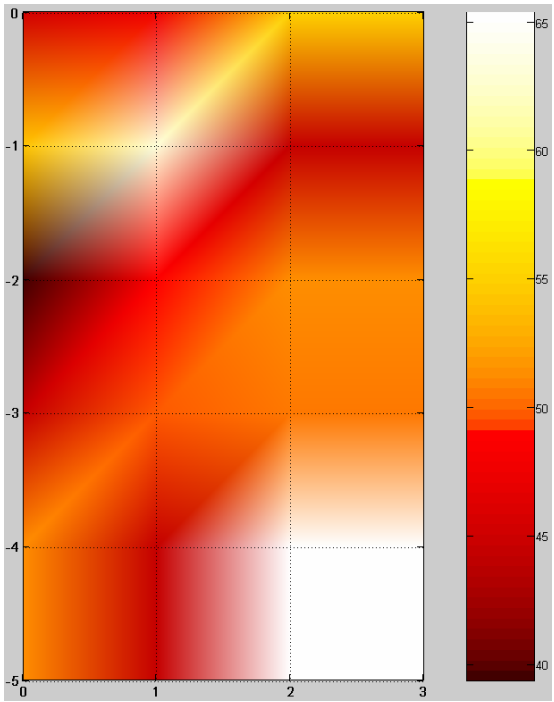
0
-1
-2
-3
-4
-5
0
1
2
3
65
60
55
50
45
40

E(L)

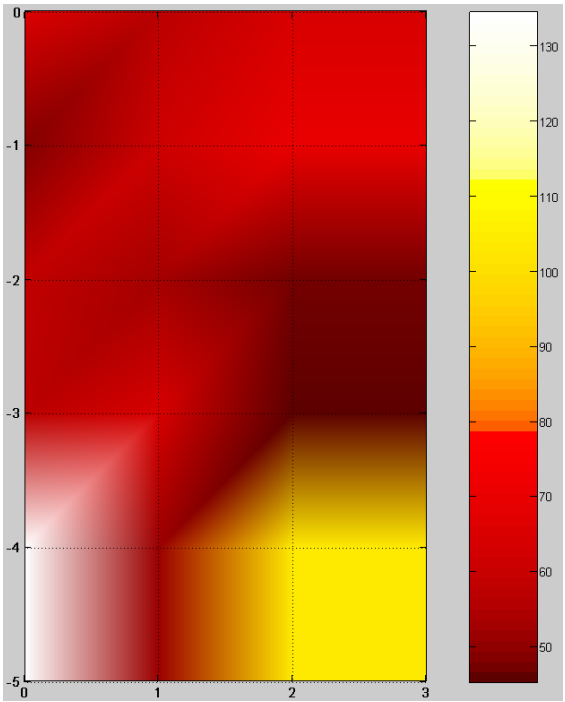
0
-1
-2
-3
-4
-5
0
1
2
3
130
120
110
100
90
80
70
60
50

E(R)

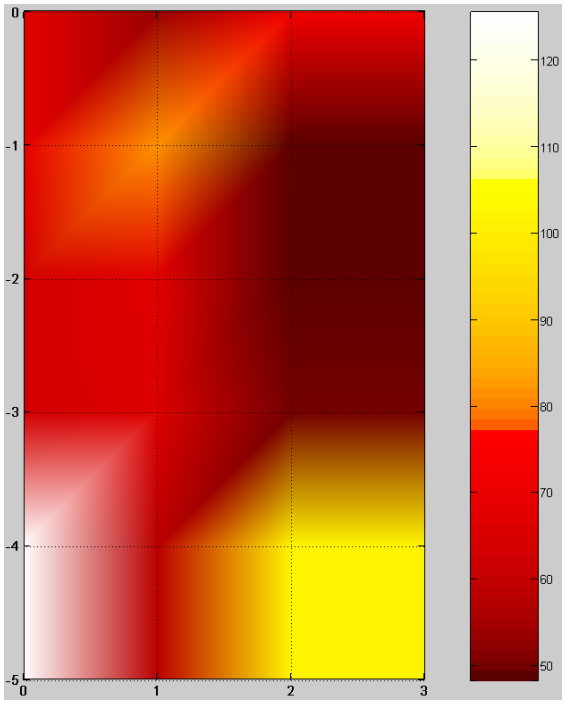
0
-1
-2
-3
-4
-5
0
1
2
3
120
110
100
90
80
70
60
50

F(L)

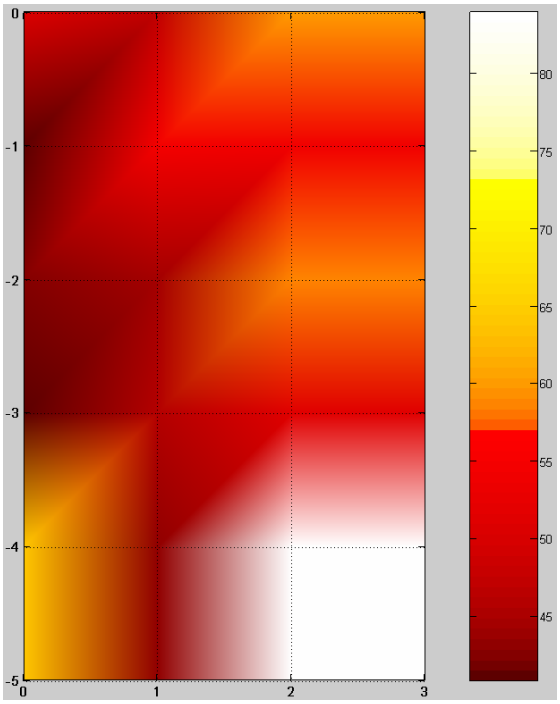
0
-1
-2
-3
-4
-5
0
1
2
3
80
75
70
65
60
55
50
45

F(R)

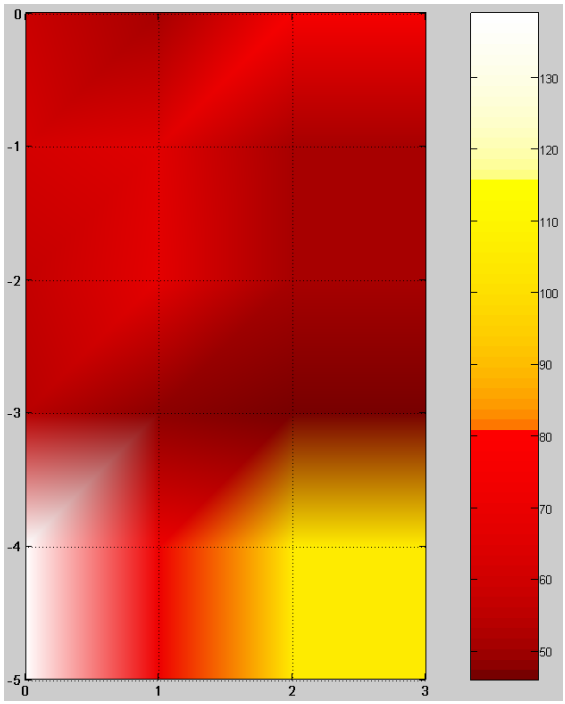
0
-1
-2
-3
-4
-5
0
1
2
3
130
120
110
100
90
80
70
60
50

G(L)

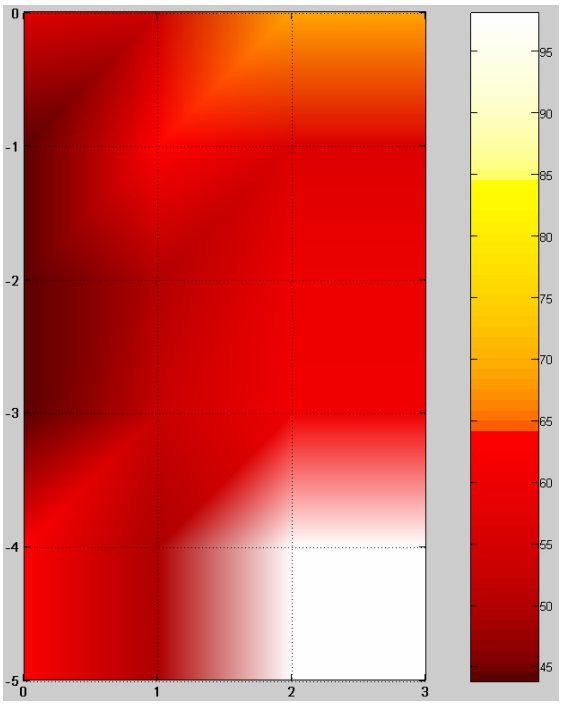
0
-1
-2
-3
-4
-5
0
1
2
3
95
90
85
80
75
70
65
60
55
50
45

G(R) H(L)

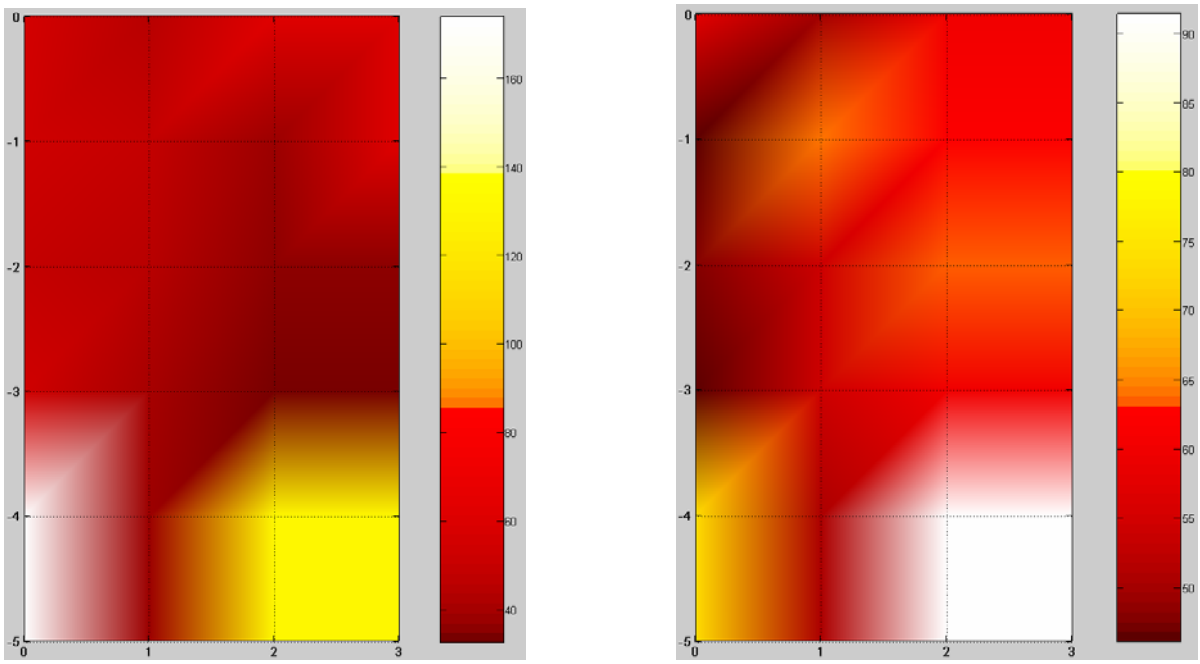

Fig. 47. Lighting panel distributions.

To summarize the observations and the results of the lighting tests:

1. It can be seen from Table 5 that light sheet A delivers the minimum amount of light (average 39.5 µmols $s^{-1}m^{-2}$). There are two contributing factors. First, as shown in Figure 45, there is a bend in the fiber coming from the collector, causing a significant amount of light to be lost before entering the light sheets. Also the longer the fiber length, the greater the loss of transmitted light before entering the light sheet.
2. Light sheets C and F deliver the maximum amount of light (average 68.9 µmols $s^{-1}m^{-2}$). This is because the fibers going into light sheets C and F are shorter.
3. It has been noticed that light intensity delivered from right side of each sheet is less than that of the left side. As shown in Figure 46, the right side of the sheets has the fixture for holding the fibers. This may reduce the light output.

In general, the lighting system performed more than adequately throughout the duration of the testing. The total system delivers light at a level to sustain a high level of growth in the algae, as will be discussed later.

Subtask 1.3 Investigate growth surface subsystem design

The growth of cyanobacterial isolates in the presence of Omnisil was studied. Initial experiments with Omnisil led to cultures dying one day after inoculation. Measurement of pH showed decrease of pH in the medium to 3. To remedy this problem we incubated Omnisil for one day in

0.1 N KOH followed by rinsing with water. Incubation of thus washed Omnisil in BG-11 medium for one day did not cause the pH (pH 8.2) to fall significantly. Testing then showed that cyanobacteria grew well in the presence of Omnisil treated with KOH, as shown in Figure 48.

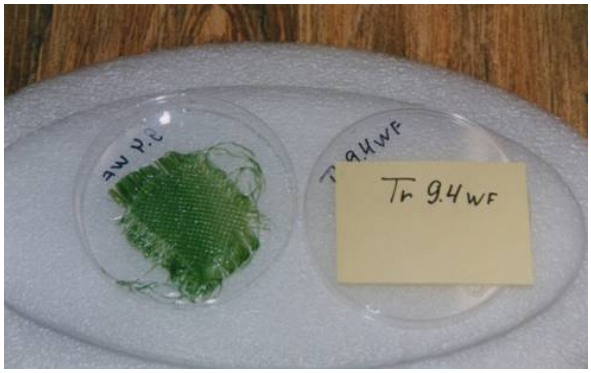

Fig. 48. Omnisil coupon populated with 9.4 WT isolate.

The growth of 2.1 (III) (*Mastigocladus laminosum)*, 8.2.1 (*Synechococcus* sp.*),* s.c.10, 1.2 s.c. 6 (*Chlorogloeopsis* sp.) and 3.3.2 (*Synechococcus* sp.*)* s.c.1 on Omnisil was then investigated, as shown in Table 6. It was found (Table 3) that only *Chlorogloeopsis* sp. was able to grow in batch culture in the presence of Omnisil, which was confirmed in a second set of experiments.

Table 6. Results of three experiments with Omnisil and new CB isolates.

Strain name	Survival Experiment 11/17/02*	Colonizing Rate Experiment 11/17/02*	Survival Experiment 12/04/02	Colonizing Rate Experiment 12/04/02	Survival Experiment 12/12/02	Colonizing Rate Experiment 12/12/02
2.1 (III) *Mastigocladus*	-	-	+/-	-	+/-	-
8.2.1 Trich. Cord *Synechococcus* s.c. 10	-	-	+/-	-	+/-	-
3.2.2 *Synechococcus* s.c. 1	-	-	+	+	+	+
1.2 *Chlorogloeopsis* s.c. 6	+	+	+	+	+	+

* The negative results of the experiment of 11/17/02 might be connected with a high level of illumination.

Following the experiments, the growth flasks were covered by window screening to see if the negative effect of Omnisil could be reduced at lower light levels. It was found that the cultures 3.2.2 *Synechococcus* s.c. 1 and s.c.1.2(6) *Chlorogloeopsis* were able to grow in the presence of Omnisil and colonized this substratum under moderate illumination. It seems reasonable therefore to screen all cultures for their ability to grow on Omnisil *before* embarking on a program of physiological studies. Such studies would become redundant if in fact the cyanobacteria were not able to grow in the presence of Omnisil, which at the moment, is still the

prime candidate for use as a substratum in the CRF. Note that in contrast to the enrichments made from Scotch Brite, these isolates were not initially made from Omnisil placed in the field. The mechanical strength of this material did not allow us to leave them *in situ*. Further, some of the areas sampled were mineral-precipitating regions and thus the substrata quickly became engulfed in the mineral. These experiments were performed with a new batch of Omnisil and it was washed as before. The pH of water after autoclaving with Omnisil is close to neutrality, so no contamination with acid was found as in the earlier work.

The effect of Omnisil coupons prepared by Ohio University on the growth of *Chlorogloeopsis* sp. in BG-11 medium supplemented with 30 mM HEPES and aerated with 5% CO_2 in air was studied. Although the inoculum level was low, *Chlorogloeopsis* sp. grew well in the presence of Omnisil coupons prepared in Ohio, as shown in Figure 48. The coupons decreased medium pH to 6.7, while CO_2 aeration alone decreased pH to 7.4 Coupons soaked in BG-11 medium with 30 mM HEPES reduced the pH of the medium from pH 7.85 to 7.15.

The pH dynamics of two cultures were compared with the planktonic culture (dark blue curve) and the culture grown on the Omnisil. This suggested that Omnisil coupons treated in Ohio decreased medium pH significantly. The result of the acidification is that there was almost no planktonic fraction of cyanobacteria when grown in the presence of Omnisil, as shown in Figures 49 and 50. This was confirmed by separate determination of chlorophyll "a" amount on Omnisil coupon and tube walls, shown in Figure 51. Planktonic chlorophyll was not detectable.

Fig. 49. Colonized Omnisil coupons after 96 hours. Tube 1 (left), planktonic; tubes 2 and 3, Omnisil.

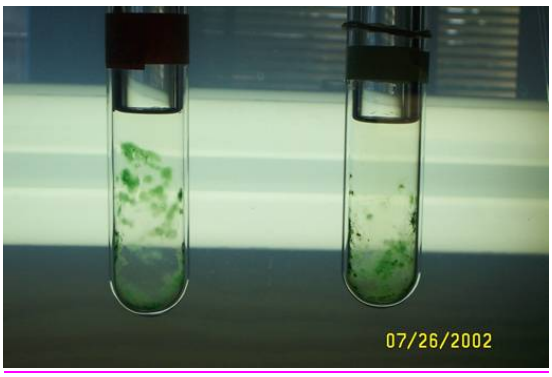

Fig. 50. Growth tubes after removal of the Omnisil. Note the absence of a planktonic phase.

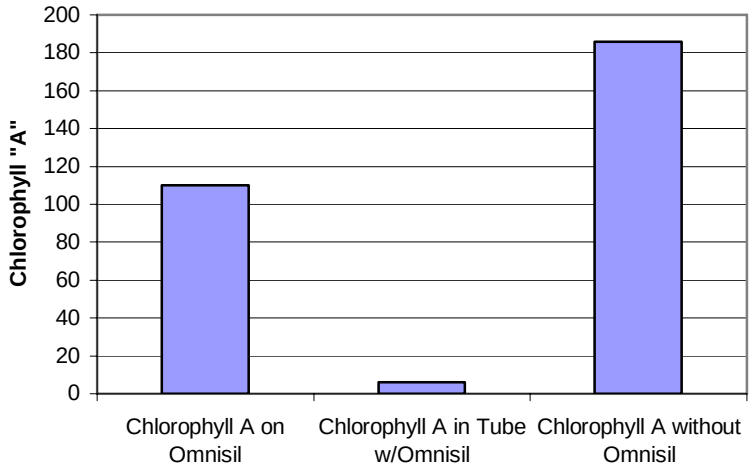

Fig. 51. The distribution of chlorophyll (as cyanobacterial biomass) between Omnisil coupon and tube walls. Last column on the right shows the yield in tubes without Omnisil coupon**.**

Figure 51 suggests that 93% of cyanobacterial biomass was concentrated on the Omnisil coupon. In the absence of Omnisil, there was no wall growth. The difference between chlorophyll yield in tubes with and without coupons may be explained by shading in tubes with coupons.

Subtask 1.4 Investigate the use of a hydraulic jump to improve the system's overall CO_2 conversion efficiency

CO_2 scrubbing tests were carried out to understand the CO_2 scrubbing capability of translating slug flow under various conditions. The liquid velocities for the test range from 0.6m/s to 1.0m/s and the gas velocities from 4.8m/s to 9.0m/s. The liquid used in the test is tap water. The gas consists of 15% CO_2 and 85% N_2 to simulate the flue gas in a power plant.

Subtask 1.4.1 Pressure drop test

The pressure drop tests were continued in order to understand the basic pressure drop across the translating slug flow reactor. The pressure drops were measured with respect to various liquid and gas velocities in the slug flow reactor.

One thousand data points of pressure drop of each condition were obtained by the data acquisition system. Because of the fluctuation of the pressure drop, maximal pressure drop and the average pressure of each condition were recorded. The following graphs (Figure 52) show the results of the pressure drop test. The distance between the two pressure taps for measuring pressure drop is 11.48m.

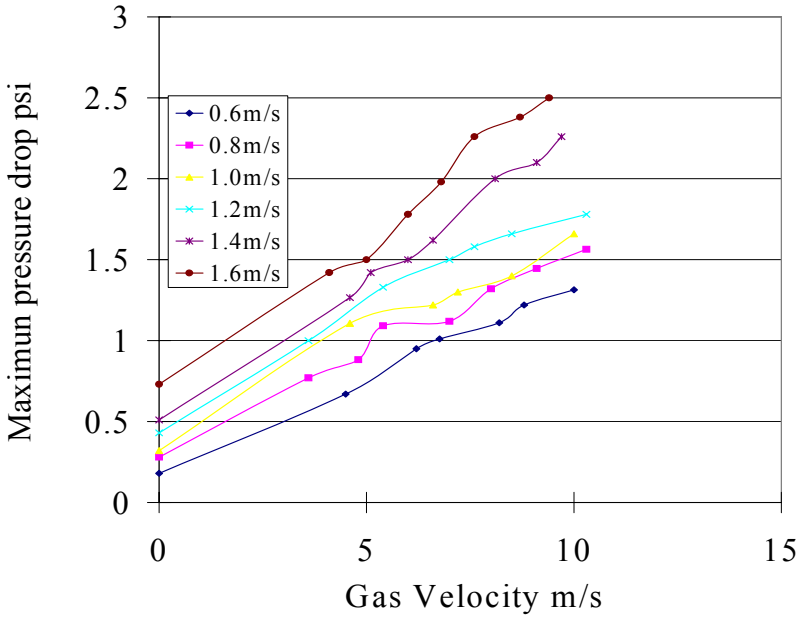

a. Maximum pressure drop

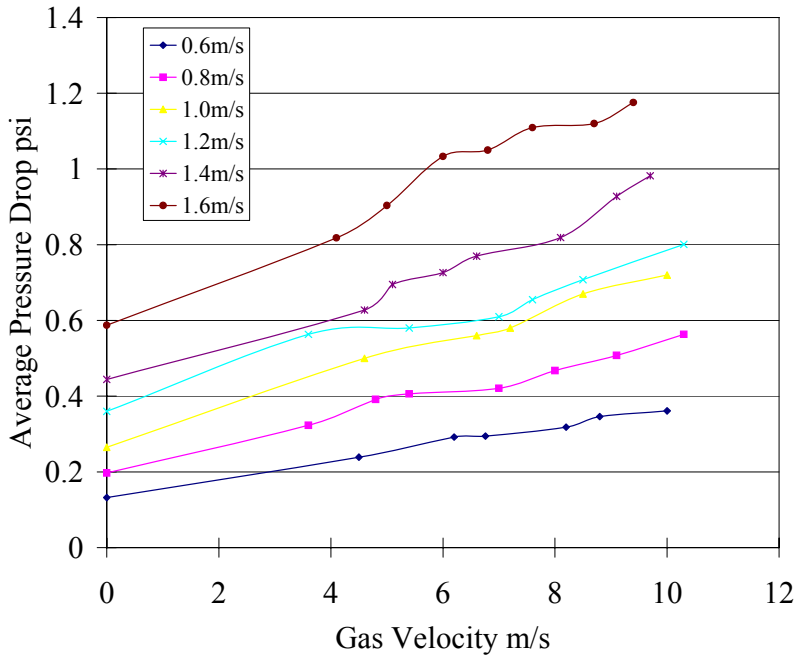

b. Average pressure drop

Fig. 52. Results of the pressure drop test.

The pressure drop of slug flow fluctuates because the slugs pass through the pressure taps periodically. Figure 53 shows the change of pressure drop with respect to time.

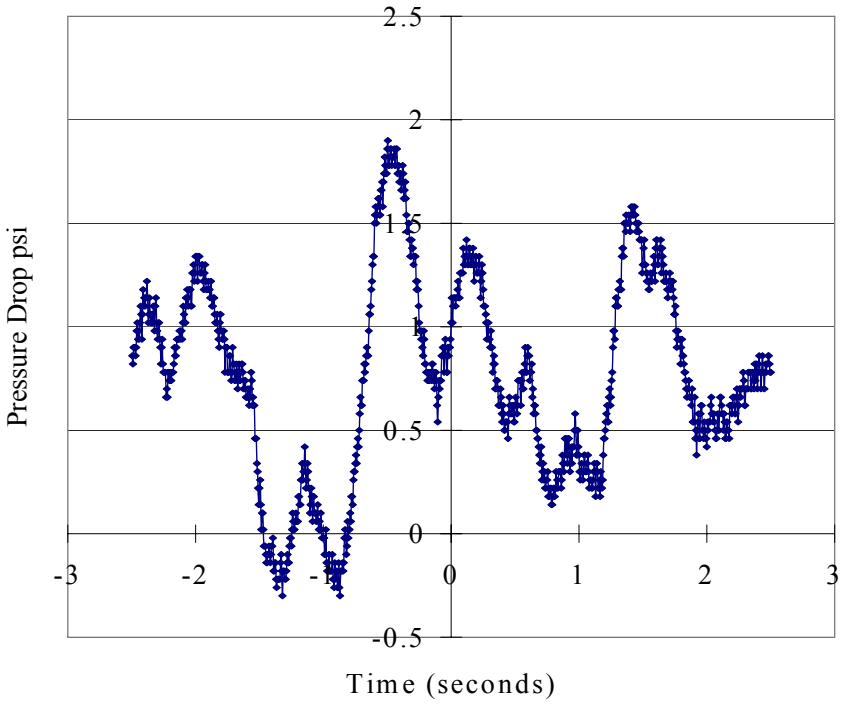

Liquid Velocity=1.0m/s, Gas velocity=10m/s.

Fig. 53. Pressure drop fluctuations.

1.4.2 Method for CO_2 scrubbing test

Liquid samples were taken at both the inlet and outlet of the reactor simultaneously. When sampling CO_2 from the pipeline, part of the CO_2 leaves the solution due to the decrease of CO_2 partial pressure. In order to prevent the sampling process from degassing, a syringe was used to withdraw the liquid sample from the slug. The sample then was slowly injected into NaOH solution so that the gas phase CO_2 could be totally captured in the solution. Finally, a titration method was conducted to measure the CO_2 concentration in the solution.

1.4.3 Test results

The CO_2 concentrations for various baseline gas and liquid flow conditions are shown in Figure 54. Figure 55 compares the CO_2 concentration increase at different gas velocities including 4.8, 6.6 and 9m/s. The result shows that when the liquid velocity is 1m/s, the CO_2 concentration increase has no obvious change. We can explain the phenomenon in two ways: one is that the turbulence inside the slug does not change a lot with the increase of gas velocity, so the mass transfer rate does not change with the gas velocity. The second explanation is that although the turbulence increases with the gas velocity, the residence time of slug decreases, causing little overall effect.

Figure 56 shows the CO_2 increase with the gas velocity when liquid velocity is 0.6m/s. The CO_2 concentration increase is less when the gas velocity is 4.8m/s because the turbulence in low gas velocity is not as intense as at higher velocity, causing lower mass transfer rate.

Liquid Velocity 0.6 m/s Gas velocity 4.8 m/s

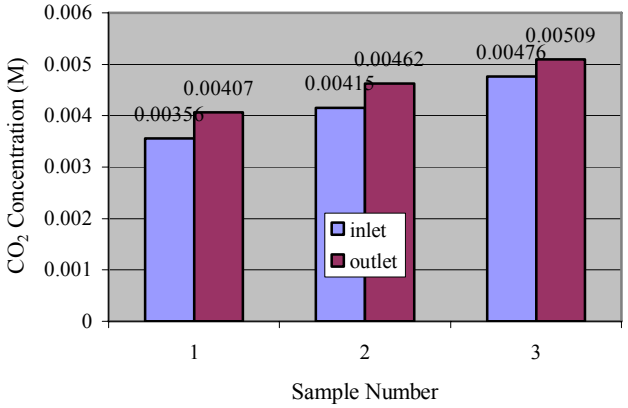

Liquid Velocity 0.6 m/s Gas velocity 9.0 m/s

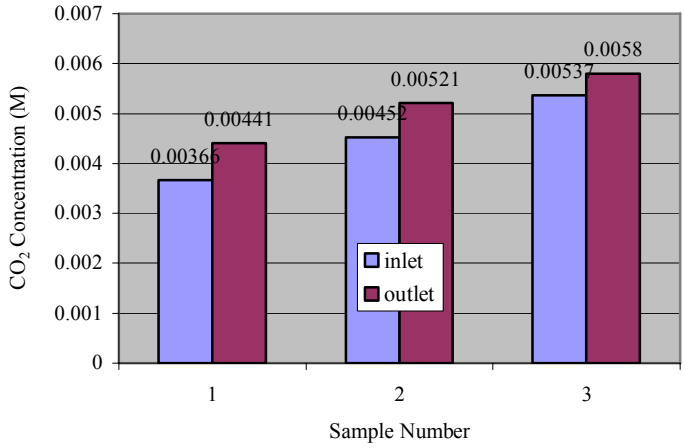

Liquid Velocity 1.0 m/s Gas velocity 4.8 m/s

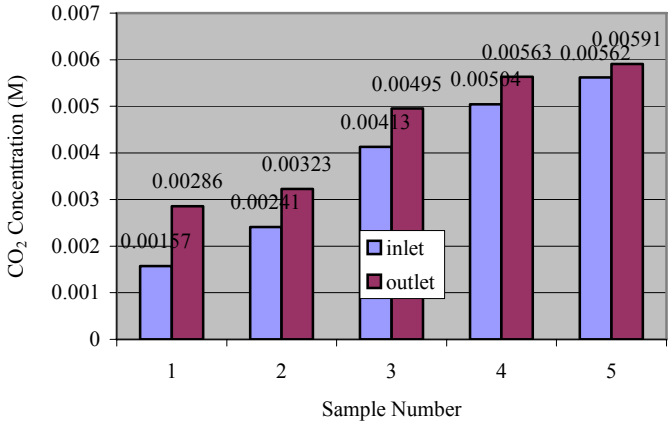

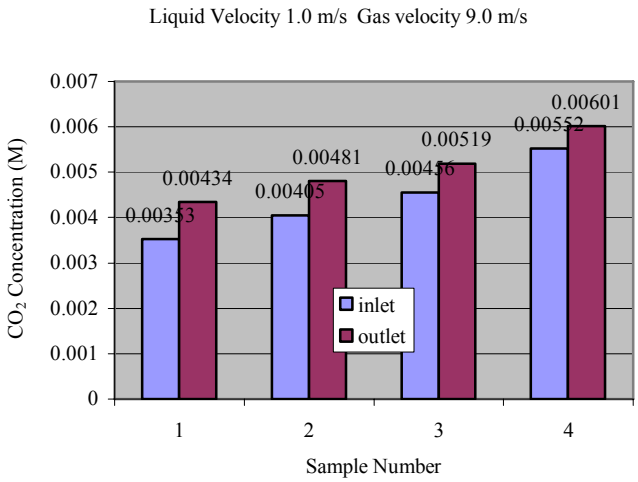

Fig. 54. CO_2 scrubbing test concentrations at several representative test conditions.

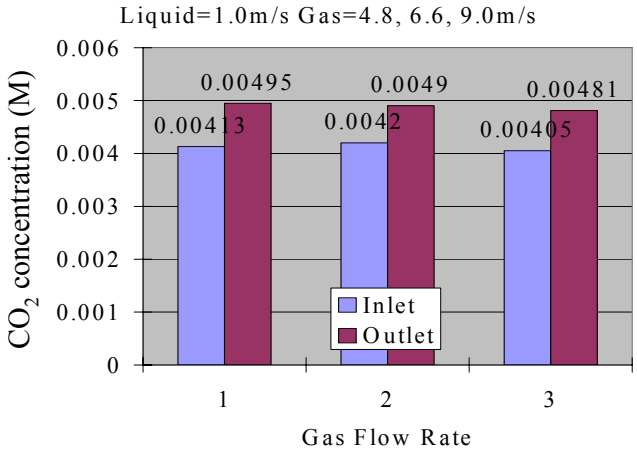

Fig. 55. Comparison of scrubbing results at 4.8 m/s.

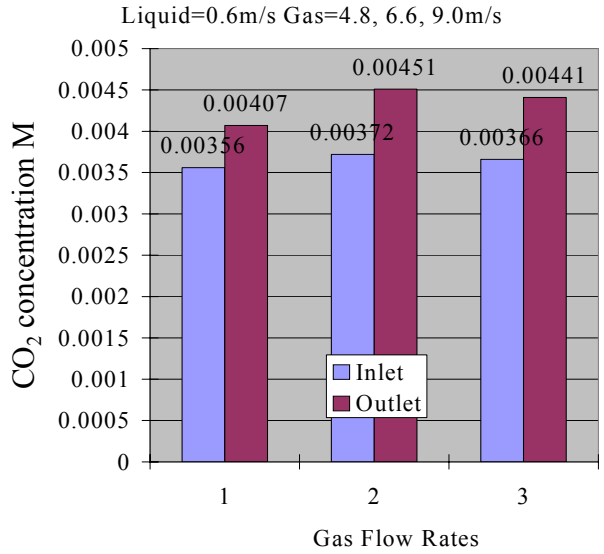

Fig. 56. Comparison of scrubbing results at 0.6 m/s.

Subtask 1.5 Design harvesting subsystem

1.5.1 Flow header design

We have completed design work for the integrated screen wetting/ harvesting system, working with Omnisil screens and s.c.1.2(2) organisms. We fabricated and tested the "Drilled-Hole Design" inserts. Initial tests conducted using water only showed that the flow across the membrane was even. In tests of the inserts using a solution containing organisms (to analyze the behavior under actual conditions) the headers performed well, providing even flow and avoiding clogging.

The insert design using shims to function as pressure and flow regulators (Figure 57) was fabricated and tested using 0.015 inch-, 0.020 inch- and 0.025 inch-thick shims. This design also showed good flow characteristics and there was no appreciable clogging noticed during and after the test. Overall it appeared that the "Pressure Manifold Design" was less susceptible to clogging than the drilled-hole design, which is an important concern during long-term testing.

To gain additional information, a comparative test was run to create a flow rate vs. pressure plot for three header insert designs (Figure 58). Notice that the performance of the 0.02" shim and the drilled hole design are very similar, and that thickening the shim has the expected effect of reducing the flow at a given pressure for the shim design, but the basic pressure-flow relationship retains the same.

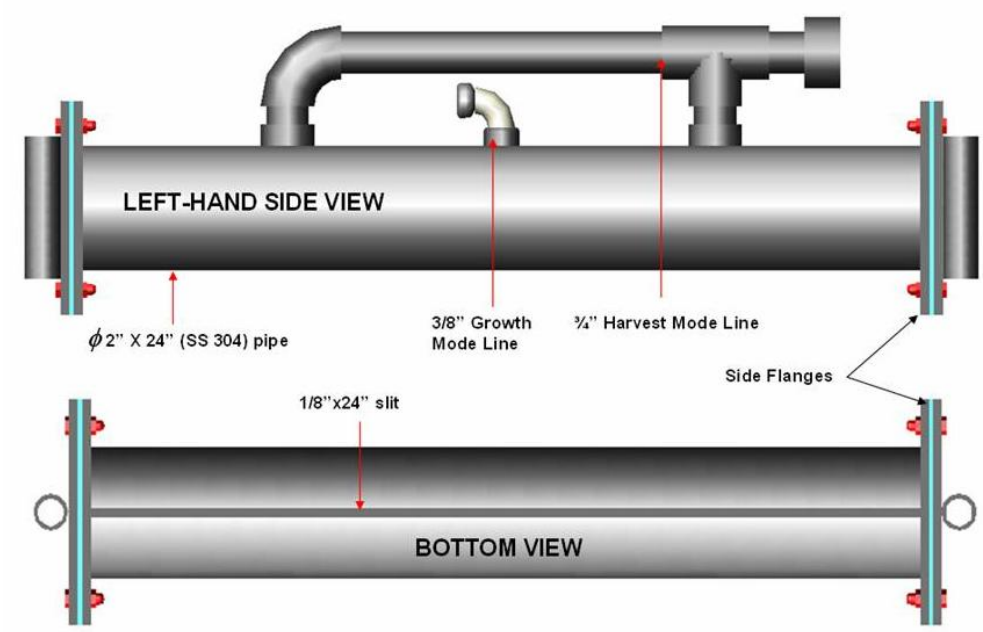

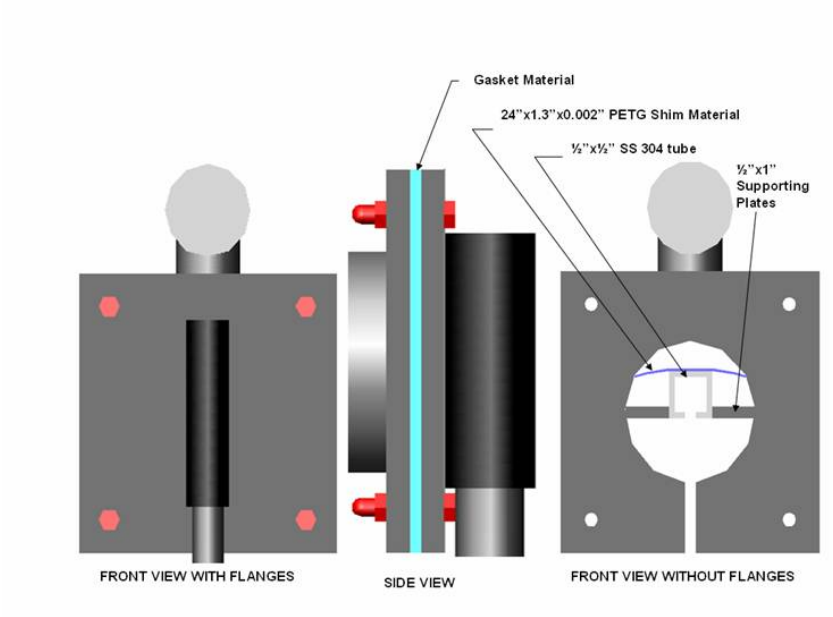

Fig. 57. Header pipe flow control inserts.

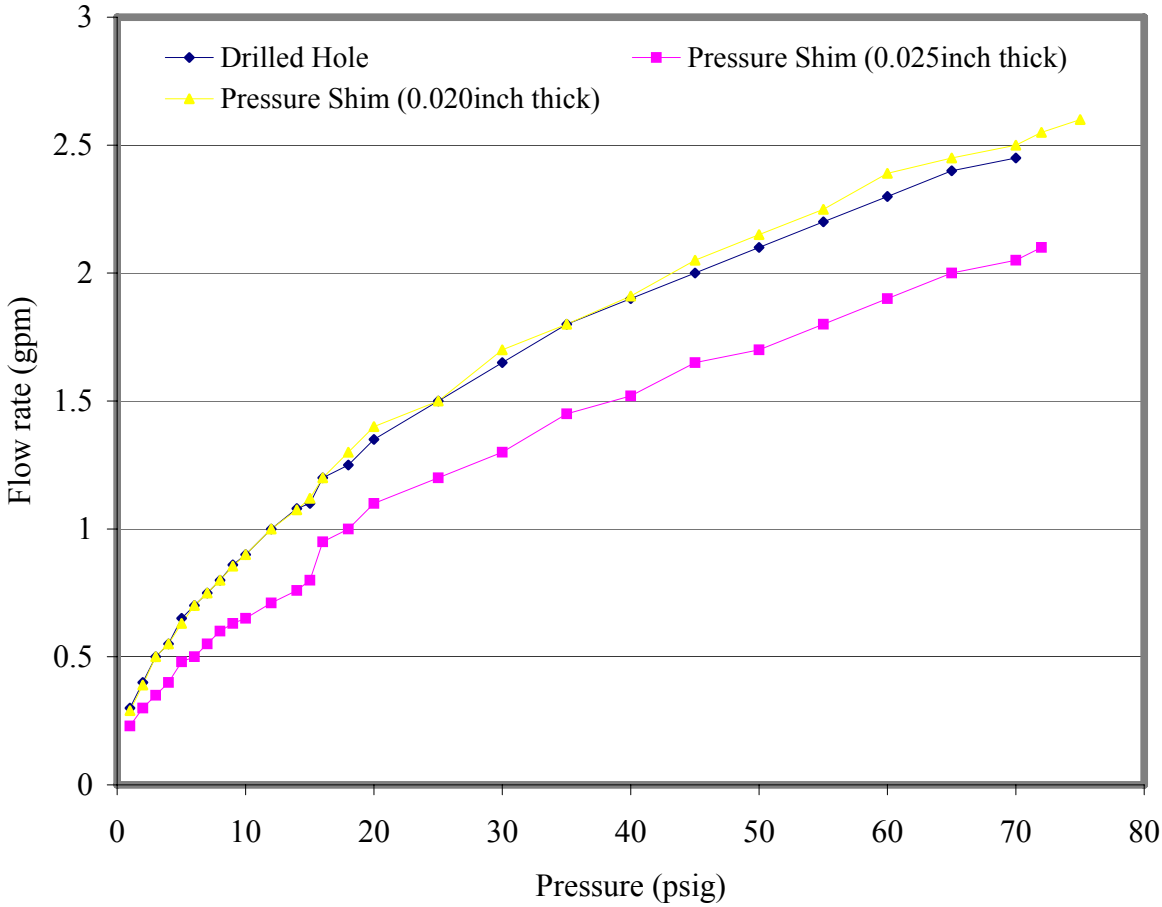

Fig. 58. Header flow characteristics as a function of water pressure.

1.5.2 CRF-2 long-term qualitative tests with harvesting and post-harvesting growth

1.5.2.1 Test 1: Using drilled-hole designed headers. Approximately 0.6 gpm flow rate was maintained during dripping mode to grow the organism. Organisms grew very well on the Omnisil membrane. They showed very good qualities of adhering to the membranes. At the end of the five-week test in the Carbon Recycling Facility Version 2 (CRF-2) we tried to harvest the organisms from the membrane by increasing the flow rate above the drip mode level. The harvesting was not a success, partly due to mechanical problems with the header pipes. The headers had been manufactured from clear plastic to allow visualization of the flow control system within the header pipe, but the holes drilled and tapped into the brittle plastic for the water lines developed edge cracks so the pipes would not hold pressure for the harvesting mode. The headers for the next test were made from a less brittle PVC material to avoid this problem.

1.5.2.2 Test 2: Using pressure shim headers. Another long-term test was started and is still continuing. The dripping mode was a success and the organisms adhered well to the membrane. The flow rates were approximately 0.5 gpm. After sufficient growth was established on the screens (after several weeks), we performed a harvesting test by increasing the flow on one of the membranes, but we were unable dislodge a substantial amount of organisms from the membrane. The flow that we were able to achieve was only 2 gpm with the test system, and there was not a full "sheeting action" as desired for harvesting. These test results show that a higher flow may be necessary for harvesting and that the test system will have to be modified to achieve a higher flow for future harvesting tests. Figures 59 and 60 show the screen on both sides before and after harvesting.

To quickly test if harvesting could be achieved using this type of header design modified to allow higher harvesting flow rates, we simulated the "sheeting action flow" (no impingement jet) by removing the inlet water pipe from the header and using the full flow rate on a small area of the screen. In this test we were able to dislodge an appreciable amount of the organism from the "harvested" section of the membrane. The flow rate was 1.55 gpm, and it was directed to the left 1/3 of the screen width on one side of the screen only (side B). The results of this test, shown in Figures 61 and 62, indicated that harvesting was possible using only high-flow sheeting action (no impingement jet is needed), but we estimated that 5-10 gallons per minute was needed to achieve the desired level of harvesting for the entire screen.

The design changes to the overall test system required to produce the high flow rates needed for harvesting were completed and tested. The flow to the header for the existing test system was limited by the fluid inlet tube, so it was modified to have a maximum flow capacity of 10 GPM while still maintaining the low flow capacity for growth mode. The changes to the system included manufacturing new header/frame units out of stainless steel material with increased flow capacity and a modified pipe end sealing method to improve flow uniformity, identifying and purchasing a new high flow harvesting pump and plumbing it into the system, and improving the test system data acquisition unit. Qualitative system tests showed that the harvesting system performed wonderfully, cleaning the growth surfaces within a matter of seconds.

We were also successful in growing organisms on the "cleaned" section of the membrane after the harvesting, as shown in Figure 63. This indicates that continuous bioreactor operation is feasible, with continuous cycles of harvesting and repopulating screens.

a. Before harvesting test

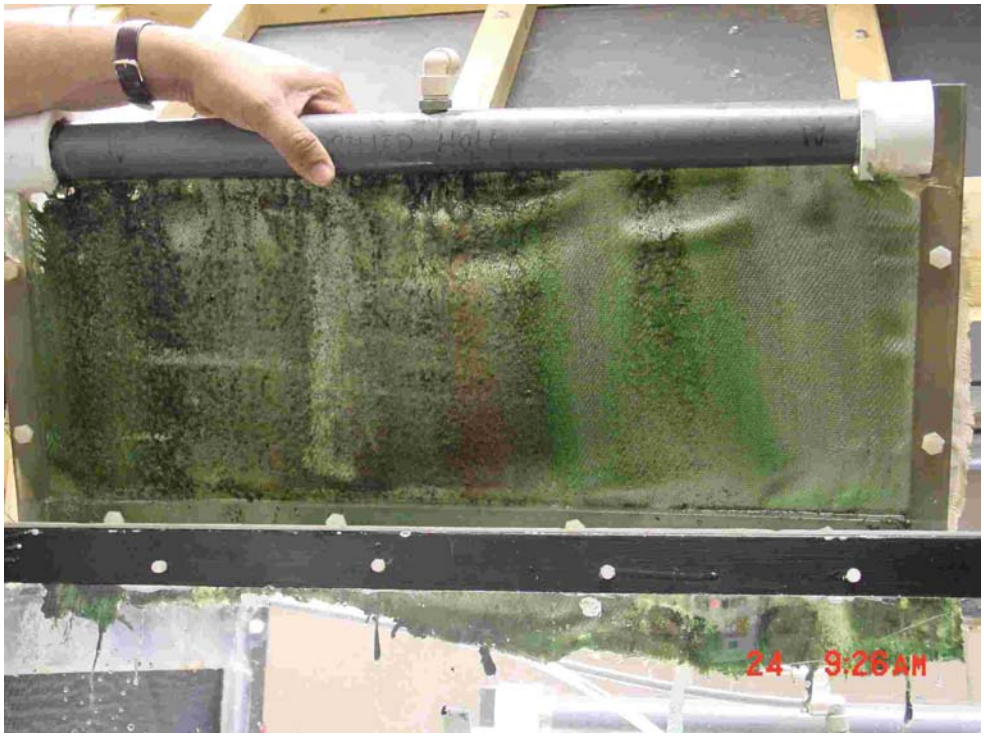

b. After harvesting test

Fig. 59. Screen side A before and after harvesting with 2gpm flow through the header.

a. Before harvesting

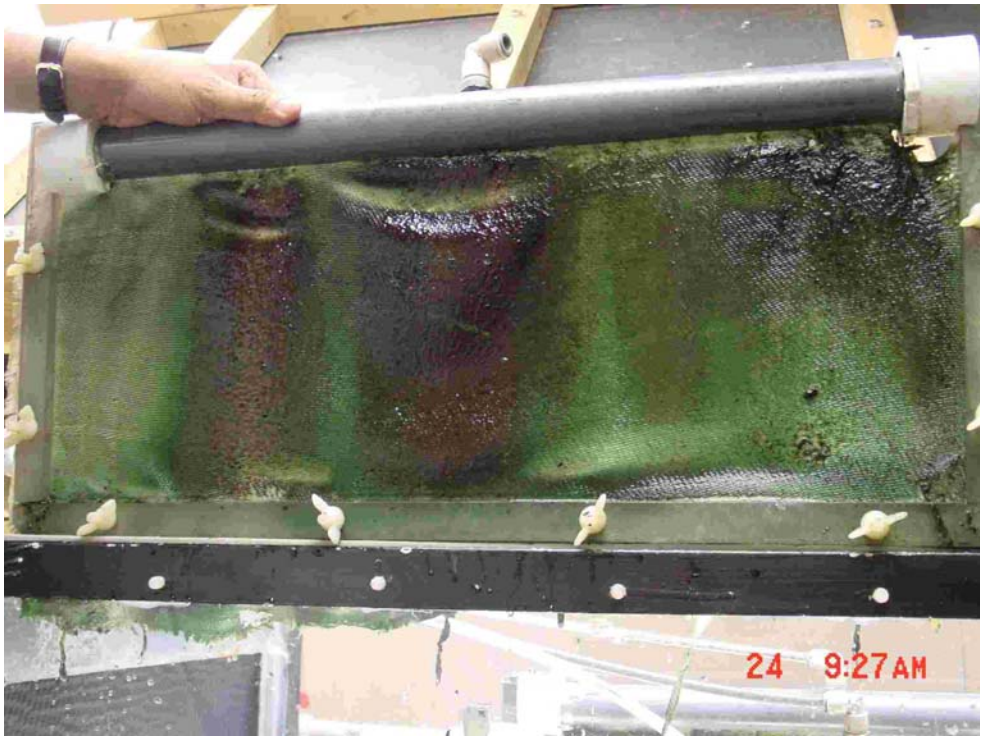

b. After harvesting

Fig. 60. Screen side B before and after harvesting with 2gpm flow through the header.

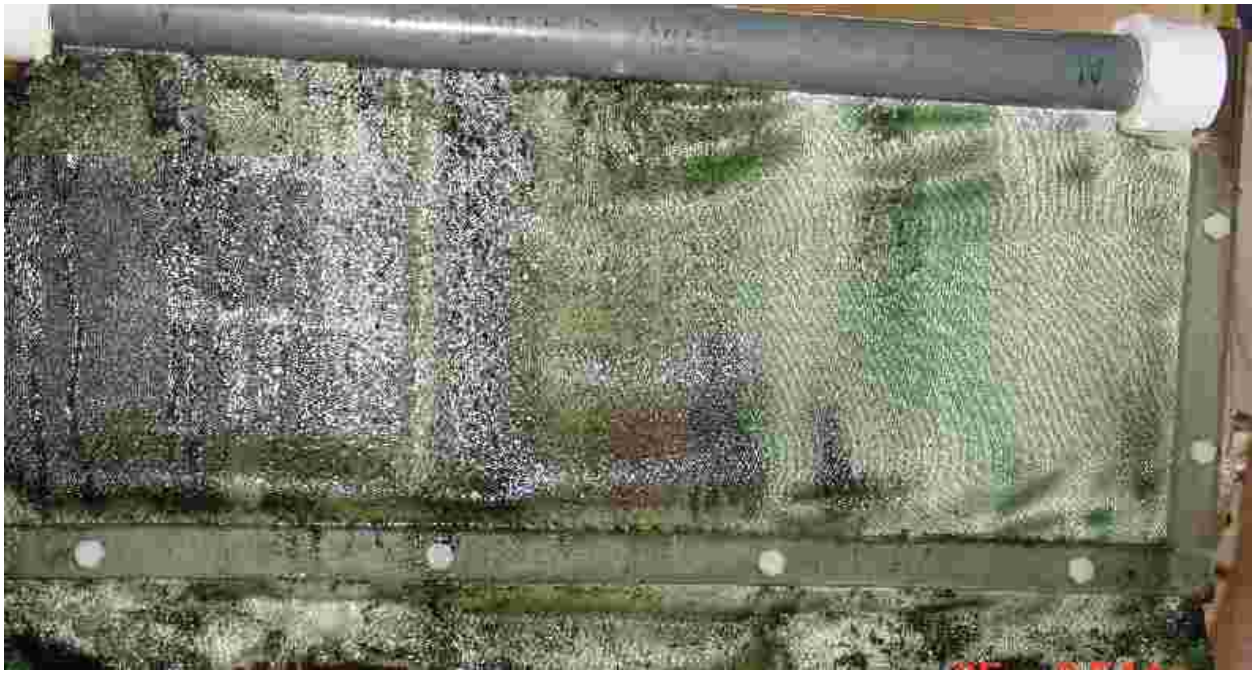

a. Side B before harvesting

b. Side B after harvesting

Fig. 61. Screen side B before and after harvesting with 1.55 gpm.

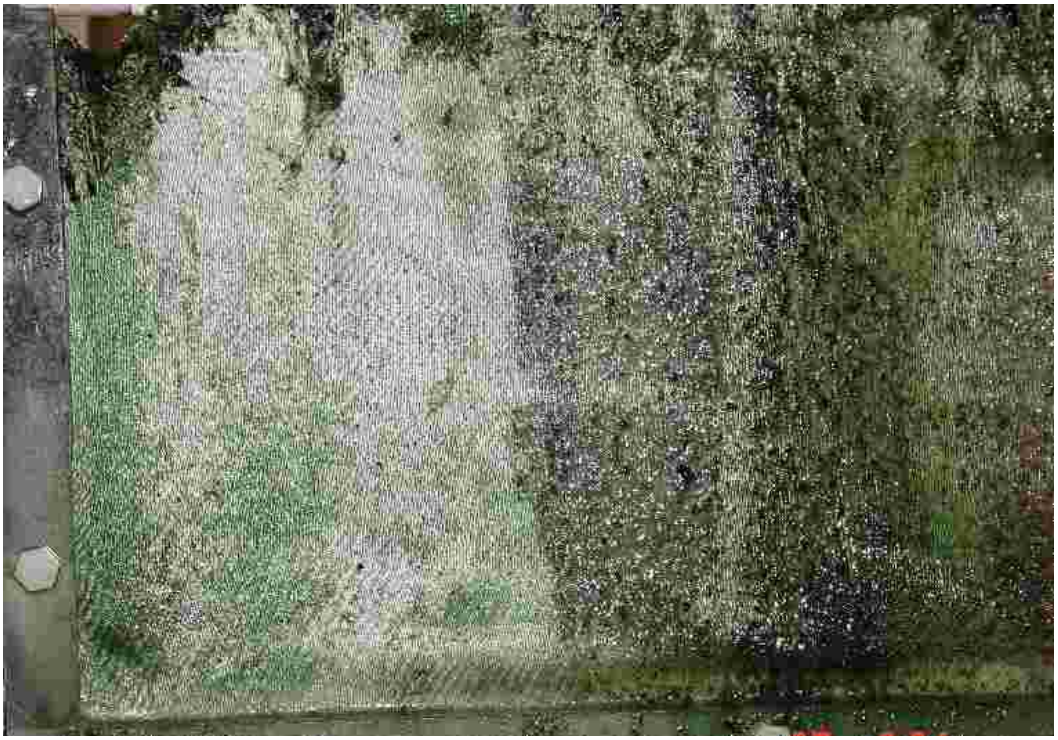

Fig. 62. Side B after local harvesting (close up).

Fig. 63. New growth in harvested area.

Subtask 1.6 Quantify properties (higher heating value, elemental composition, volatile content) of dried biomass for potential end-uses

The technical aspects of bioreactor operation and biosequestration appear to be either solved or indicate they are attainable in a larger-scale reactor. This question, however, of what to do with the algae after it is harvested, has turned out to be key to commercialization. We see a huge potential for refining harvested biomass into transportation fuels. Given the cost of petroleum-based fuels, we believe there may be a market for a closed system bioreactor to allow the U.S. to produce transportation fuel using a renewable resource.

Certain algal strains produce a significant fraction of lipids, as identified by the Department of Energy's Aquatic Species Program: Biodiesel from Algae (NREL/TP-580-24190). Many economists, engineers and biologists have long speculated that microalgae could be the answer to stimulating biodiesel production. Yet, despite years of research funded by DOE (NREL), the answer has not evolved.

For many reasons, researchers have failed to create systems for producing continuous quantities of microalgae suitable for biodiesel production. While development of rapid growing strains that generate high mass fractions of lipids met with some success, almost all attempts at growing these specifically engineered or isolated strains in large raceway cultivators has met with contamination and domination by native species. Further, where there is plenty of land and sunlight (i.e. Western U.S.), there is a significant lack of water. Where there is abundant water, land cost is high and often simply not available for algal production facilities. Finally, even where there is abundant land and sun, the optimal level of photosynthetic radiation is usually between 1000-1500 (solar time), with much lower productivity throughout the day as the sun moves across the sky, increasing the solar angle incident from normal.

However, if a closed system bioreactor could be developed to keep the selected strain(s) isolated from the environment, to control the environment to specifically optimize delivery of photons, to enhance growth rate and lipid production, to minimize water and land usage, and to do it in a sustainable and inexpensive fashion – it could be possible to do large-scale "farming" of microalgae as an energy crop for production of biodiesel.

Closed-system production of microalgae could revolutionize biodiesel and provide stability to many agricultural markets. Current biodiesel production relies on feedstock crops. These are often more valuable as food for humans and livestock and these crops produce only small amounts of fuel per acre, typically less than three barrels per acre per year. The use of a closed-system bioreactor to grow microalgae could provide a constant supply of biomass for the commercial production of biodiesel. In addition, once the biorefining industry was well established, it would provide a virtually limitless demand for any crop that could be used in the production of biodiesel. For example, should a harvest be so bountiful as to push the price of soy below the level where biodiesel can match the price of petro-diesel, the biodiesel producers could enter the market and boost the price of soy to that level. This would create additional crop sales and could create substantial new income for farmers. Further, it would create stability in the pricing markets, giving farmers needed security.

Task 2.0. Evaluate subsystem combinations and select an "optimum" system design

Most of Task 2 was incorporated into the results for Task 1 and Task 3. The subsystem integration was completed and discussed in the results in Task 3.

Task 3.0. Implement the optimum system in scaled model

3.1 Final System Design

A final bioreactor design, shown in Figure 64, was completed and built at 1005 E. State St. in Athens Ohio, where it was tested. The results of productivity testing, shown in Figures 65 and 66, indicate the viability of the process.

The test facility was designed to simulate the flue gas emission from fossil-fired power plants and to study the effects of change in temperature, gas flow rate, pH value, nutrition concentration and CO_2 concentration in simulated flue gas on the growth ability of microalgae species. This assembly assists in reducing the pressure drop of flue gas and increases the effective area for efficient trapping and bioconversion of CO_2 in the flue gas. Eight light panels were used to illuminate over 200 ft^2 of algal growth substrates.

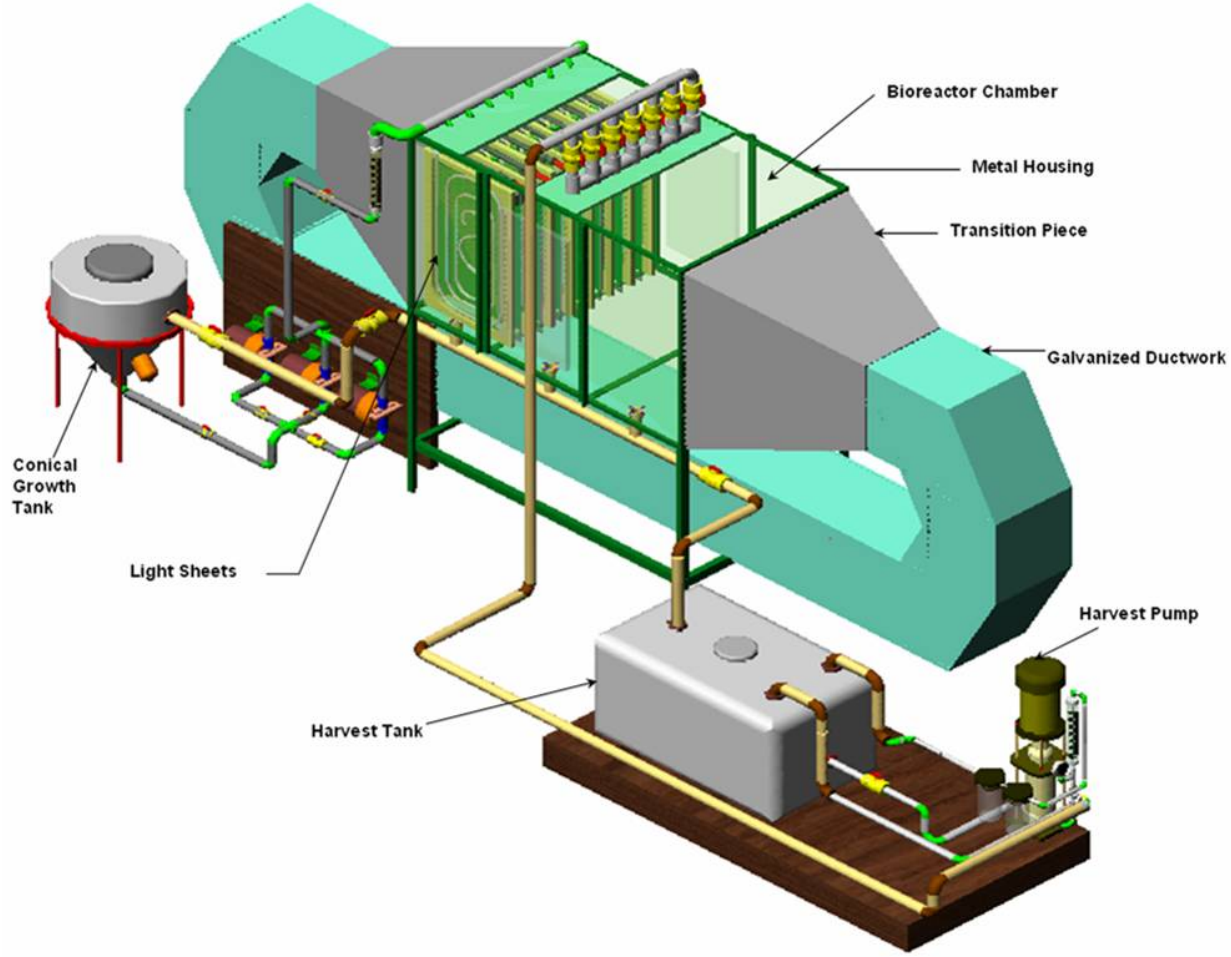

Fig. 64. Bioreactor facility (final design)

3.2 Algal productivity

Sustainability tests with approximately 30 gallons of a specially isolated strain of *Chlorogloeopsis* and two Omnisil membranes were performed to quantify the growth of cyanobacteria in the bioreactor. After completing the initial mass determination, which enabled us to quantify the cyanobacterial growth over the course of the experiment, the system was allowed to reach steady conditions (five days) before experimentation.

The daily yield of cyanobacteria was determined by harvesting each night. The harvested cyanobacteria were pumped through a 5-micron filter, which was dried for 7 days in a convective oven at 90ºC. The mass results of the daily harvesting are shown in Figure 65. Also shown in Figure 65 is the average (daily) solar flux for Athens, Ohio, during the experiment as measured at Scalia Laboratory, Ohio University's weather station.

We noted that the productivity for the following day tracked the average solar flux for the previous day's growth very well (correlating to over 98%). While not confirmed in this work, it seemed intuitive that if the solar collector/distributor system is tuned to produce an optimal photon flux (≈100 $\mu molm^{-2}s^{-1}$), then reducing the daily photon exposure would correspondingly reduce biomass productivity.

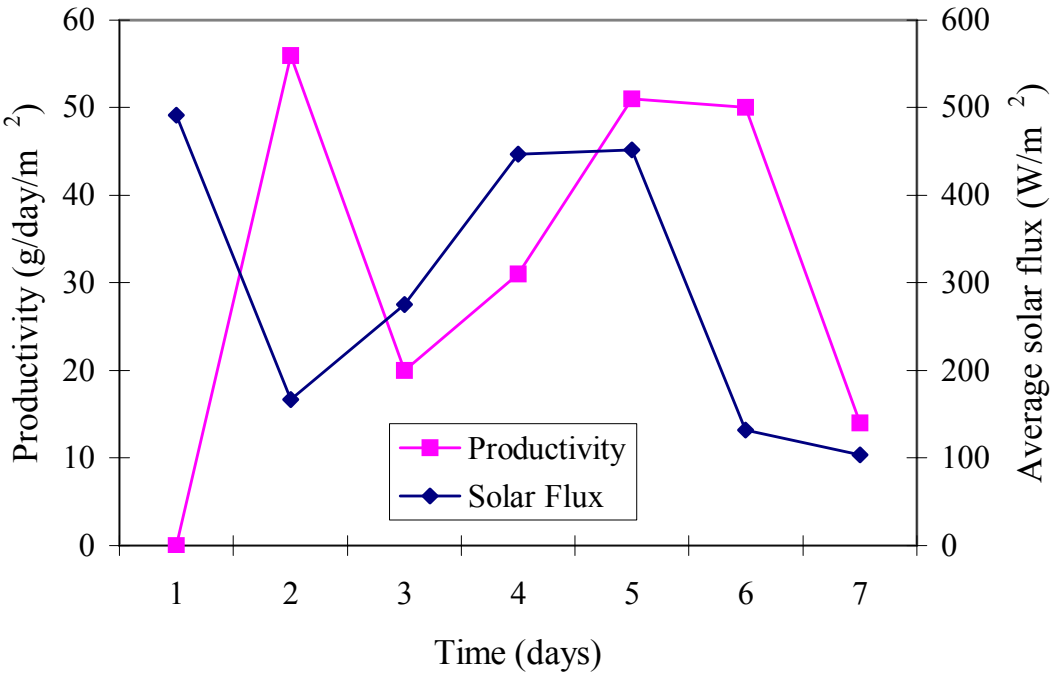

Fig. 65. Preliminary productivity data.

The tests were repeated for cyanobacterial growth over a period of ten days following an acclimation period of seven days. The results, shown in Figure 66, were slightly lower than the results presented in Figure 65, especially when normalized to the average solar flux from the day before. This is likely because the solar collector experienced significant loss of reflective coating

between May and July. However, these results are significant because they show the cyanobacteria have a considerable ability to grow once acclimated to the membrane substrate.

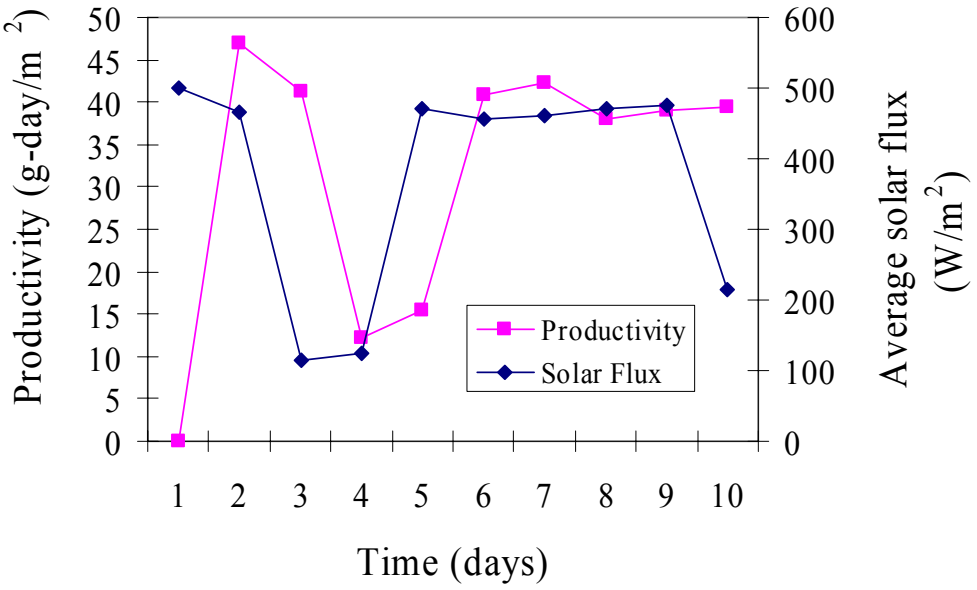

Fig. 66. Repeated productivity results.

Conclusions

Projected Costs and Benefits

Several benefits, in addition to CO_2 mitigation, could result from this novel method of photosynthetic carbon conversion. Obviously, one advantage would be the generation of O_2 as a byproduct of photosynthesis. Another potential benefit would be electrical power generation. By using filters capable of separating the infrared region of the spectrum coupled to the solar photon collection and delivery system, the infrared portion of the spectrum could be directed to photovoltaics, which use the heat to generate direct-current electricity.

Another anticipated benefit would be the reduction of additional gaseous pollutants including NH_3 (that slips through selective catalytic reduction for NOx control) and NOx (nitrogen oxides) that form from the combustion process. Work by Nagase *et al.* (2001) demonstrated considerable nitrogen assimilation from NOx species bubbled through a bioreactor and it is well established that NH_3 is an excellent source of nitrogen for many photosynthetic organisms.

Finally, the resulting biomass has numerous beneficial uses. In addition to being a potential fuel, microalgae have been used as soil stabilizers; fertilizers; in the generation of biofuels, such as biodiesel and ethanol; and to produce H_2 for fuel cells. In recent tests, it also has shown several positive ignition characteristics for cofiring with coal in pulverized coal-fired generation units.

Expected Cost of Deployment

For the purpose of this analysis to calculate the cost of removing CO_2 from the flue gas by algae, we assumed the photobioreactor would be deployed at a power plant with a gross capacity of 200 MW, a capacity factor of 65% operating as a load-following unit (peaking during the day when solar photons are available), with a heat rate of 9000 BTU/kW-hr, burning a coal containing 70% carbon by mass and a higher heating value (HHV) of 12,000 BTU/lbm. The bioreactor for this economic case study is assumed to remove 50% of all CO_2 during daylight hours (during peak CO_2 production), and the incident photon flux on the solar collectors as delivered to the bioreactor is 1200 μmols m^{-2} s^{-1}. This value assumes that the only significant decrease in photon flux is not solar angle (overcome by mirror positioning), but cloud cover.

It should be noted that the key cost parameter is the cost of the solar collectors. It is estimated that the collectors, built by hand, would cost $30,000 apiece to install. Without mass production and economies of scale, $30,000 per collector would translate to $2,000 per ton of CO_2 removed from the flue gas by the algae. However, commercialization and mass manufacture of the solar collector technology is likely. The design team, headed by Oak Ridge National Laboratories, has received funding from DOE to further its hybrid lighting work. This technology is focused on use as a lighting system in commercial buildings. The current cost goal for the team's *building system* is $2,000/$m^2$ for light collecting.

In order to examine the effect of photon conversion efficiency at a collector cost of $2,000/$m^2$, Figure 67 was generated. Using the previously stated assumptions, the minimum cost for collection of one ton of CO_2 by algae over the lifetime of the bioreactor, assuming continuous

use, would be $80. Even assuming an extremely optimistic 30% conversion efficiency, the more likely cost is $240 per ton of CO_2 removed from the flue gas by the algae – *with no revenue generated from the resulting biomass.*

However, members of the research team are working to adjust the building-based lighting system design to a bioreactor system design, employing solar collecting troughs and optic sheets instead of optic wires. The larger collection area and elimination for the need of several separate controllers drives the estimated cost of the unit to $400/m^2 of light collecting area. In that case (labeled as "proposed design"), the economics are very favorable ($48 per ton of CO_2 removed by algae) if one assumes 30% conversion efficiency. Even if 20% conversion is reached, the cost is less than $90 per ton of CO_2 removed from the flue gas by the algae.

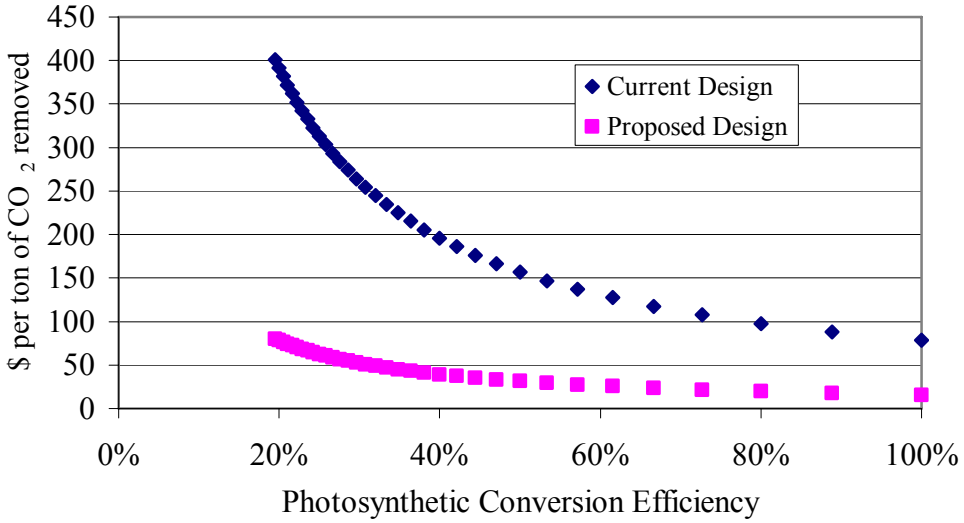

Fig. 67. Cost of one ton of CO_2 removed by algae as a function of photon conversion efficiency.

If photon attenuation is reduced and deployment of such a unit occurs in a "sunnier" location, the incident photon level could increase to approximately 1500 µmols m^{-2} s^{-1}; the cost of CO_2 removal (per ton removed by algae) for a conversion efficiency of 30% would become $39.

General Conclusions

As we finish this project, we can report that we have made significant progress toward achieving our overall project goals. Most importantly, we have demonstrated that microalgae can be grown in a harsh simulated flue gas environment to sequester carbon. And it can be done repeatably and with a high degree of solar efficiency.

The subsystem research has progressed to the point that a viable pilot-scale bioreactor is being constructed to test long-term, sustainable and continuous conversion of CO_2 to biomass using collected solar photons. Further, this photobioreactor offers numerous possibilities for not only greenhouse gas mitigation, but for control of a wide variety of pollutants, notably NOx and ammonia slip, while yielding a product that could have sustainable economic value. That product could be extremely useful in the production of domestic transportation fuel.

The productivity data strongly indicate that the harvesting method of higher water flow does not physically stress the cyanobacterial mass that remains on the substrate. This finding is critical for long-term sustainability. Further, the data reflect that productivity, at least in the current implementation, is a function of photon availability. Thus, it is seems logical that deployment should be favored in locations with higher average incident solar flux.

Finally, the economics of implementation are a significant hurdle to commercialization. Particularly, the cost of the solar collector and photon distribution systems will be key to providing low-cost greenhouse gas emission remediation.

References

Bacastow, R., and Dewey, R. (1996) *Energy Conversion and Management*, 37(6-8),1079-1086.

Benemann, J. (1997) *Energy Conversion and Management*, 38(Supplemental Issue), 475-479.

Brock, T.D. (1978) *Thermophilic Microorganisms and Life at High Temperatures*, Springer-Verlag, New York, USA.

Cooksey, K.E., and Wigglesworth-Cooksey, B. (1995) *Aquatic Microbial Ecol.*, 9, 87-96.

Fisher, A., (1961) *Solar Energy Research*, University of Wisconsin Press, Madison, WI, USA, 185-189.

Hanagata, N., Takeuchi, T., Fukuju, Y., Barnes, D., Karube, I. (1992) *Phytochemistry*, 31(10), 3345-3348.

Hirata, S., Hayashitani, M., Taya, M., and Tone, S. (1996) *Journal of Fermentation and Bioengineering* 81, 470-472.

Jepson, W.P., and Taylor, R.E. (1993) *Int. J. Multiphase Flow* 19 (3) 411-420.

Kajiwara, S., Yamada, H., Ohkuni, N., and Ohtaguchi, K. (1997) *Energy Conversion and Management* 38(Supplemental Issue), 529-532.

Kaplan, A., Schwarz, R., Lieman-Hurwitz, J., and Reinhold, L. (1997) *Plant Physiology.* 97, 851-855.

Maeda, K., Owada, M., Kimura, N., Omata, K., Karube, I. (1995) *Energy Conversion and Management* 36(6-9), 717-720.

Nagase, H., Eguchi, K., Yoshihara, K., Hirata, K., Miyamoto, K., (1998) *Journal of Fermentation and Bioengineering*, 86(4): 421-423.

Nubel, U., Garcia-Pichel, F., Muyzer, G. (1997) *Applied Environmental Microbiology* 63(8):3327-3332.

Ohtaguchi, K., Kajiwara, S., Mustaqim, D., Takahashi, N., (1997) *Energy Conversion and Management* 38(Supplemental Issue), 523-528.

Ramsing, N.B., Ferris, M.J., and Ward, D.M. (1997) *Applied Environmental Microbiology* 63(6): 2347-2354.